Molecular Pharmacology Fast Forward. Published on November 23, 2005 as DOI: 10.1124/mol.105.016998
This article has not been copyedited and formatted. The final version may differ from this version.
Molecular Pharmacology Fast Forward. Published on November 23, 2005 as doi:10.1124/mol.105.016998

MOL 16998

Insulin-like Growth Factor Binding Protein-2: contributions of the C-terminal domain to IGF-1 binding*

Megan M. Kibbey, Mark J. Jameson, Erin M. Eaton and Steven A. Rosenzweig

Department of Cell and Molecular Pharmacology
& Experimental Therapeutics
and
Hollings Cancer Center
Medical University of South Carolina
Charleston, SC 29425
(MMK, EME and SAR)
Department of Otolaryngology-Head & Neck Surgery,
University of Virginia Health System
Charlottesville, VA 22908
(MJJ)

Downloaded from molpharm.aspetjournals.org at ASPET Journals on April 22, 2024

Copyright 2005 by the American Society for Pharmacology and Experimental Therapeutics.

Molecular Pharmacology Fast Forward. Published on November 23, 2005 as DOI: 10.1124/mol.105.016998
This article has not been copyedited and formatted. The final version may differ from this version.

Running Title Page

a) Running title: IGFBP-2 C-terminal domain

b) To whom all correspondence should be sent:

Steven A. Rosenzweig

Department of Cell and Molecular Pharmacology & Experimental Therapeutics

Medical University of South Carolina

173 Ashley Avenue

Post Office Box 250505

Charleston, SC 29425

V: 803-792-5841

F: 803-792-2475

E: rosenzsa@musc.edu

c) Number of text pages: 46

Number of tables: 1

Number of figures: 9

Number of references: 40

Number of words in the *Abstract:* 232

Number of words in the *Introduction*: 734

Number of words in the *Discussion:* 1480

Downloaded from molpharm.aspetjournals.org at ASPET Journals on April 22, 2024

Molecular Pharmacology Fast Forward. Published on November 23, 2005 as DOI: 10.1124/mol.105.016998
This article has not been copyedited and formatted. The final version may differ from this version.

d) Abbreviations:

IGF	Insulin-like Growth Factor
IGFBP	Insulin-like Growth Factor Binding Protein
IGFBP-2F	IGF-Binding Protein-2 Fragment
IGF-1R	Insulin-like Growth Factor-1 Receptor
CHO	chinese hamster ovary
TCEP	tris (2-carboxyethyl) phosphine hydrochloride
MALDI-TOF MS	matrix-assisted laser desorption/ionization time-of-flight mass spectrometry
RP-HPLC	reverse phase - high performance liquid chromatography
DHFR	dihydrofolate reductase
BLOTTO	Bovine Lacto Transfer Technique Optimizer
BNPS-Skatole	2-(2'nitrophenylsulfenyl)-3-methyl-3 bromoindolenine
EDTA	ethylenediaminetetraacetic acid
HRP	horseradish peroxidase
PVDF	polyvinylidene difluoride
SDS	sodium dodecyl sulfate
QB-IGF-1	tetrabiotinylated-insulin-like growth factor-1
PCR	polymerase chain reaction
SDS-PAGE	sodium dodecyl sulfate-polyacrylamide gel electrophoresis
NMR	nuclear magnetic resonance
MHC	major histocompatibility complex

Downloaded from molpharm.aspetjournals.org at ASPET Journals on April 22, 2024

Molecular Pharmacology Fast Forward. Published on November 23, 2005 as DOI: 10.1124/mol.105.016998
This article has not been copyedited and formatted. The final version may differ from this version.

Abstract

Signaling by the insulin-like growth factor-1 receptor (IGF-1R) has been implicated in the promotion and aggressiveness of breast, prostate, colorectal and lung cancers. The IGF-binding proteins (IGFBPs) represent a class of natural IGF antagonists that bind to and sequester IGF-1/2 from the IGF-1R, making them attractive candidates as therapeutics for cancer prevention and control. Recombinant human IGFBP-2 significantly attenuated IGF-1-stimulated MCF-7 cell proliferation with co-addition of 20 or 100 nM IGFBP-2 (50% or 80% inhibition, respectively). We previously identified IGF-1 contact sites both upstream and downstream of the CWCV motif (residues 247-250) in human IGFBP-2 (Horney et al., 2001). To further test their contributions to IGFBP-2 function, the single tryptophan in human IGFBP-2, Trp 248, was selectively cleaved with BNPS-skatole and the BNPS-skatole products IGFBP-$2_{1\text{-}248}$ and IGFBP-$2_{249\text{-}289}$, as well as IGFBP-$2_{1\text{-}190}$ were expressed as GST-fusion proteins and purified. Based on competition binding analysis, deletion of residues 249-289 caused a ~20-fold decrease in IGF-1 binding affinity (IGFBP-2 EC_{50} = 0.35 nM and IGFBP-$2_{1\text{-}248}$ = 7 nM). Removal of the remainder of the C-terminal domain had no further effect on affinity (IGFBP-$2_{1\text{-}190}$ EC_{50} = 9.2 nM). In kinetic assays, IGFBP-$2_{1\text{-}248}$ and IGFBP-$2_{1\text{-}190}$ exhibited more rapid association and dissociation rates than full length IGFBP-2. These results confirm that regions upstream and downstream of the CWCV motif participate in IGF-1 binding. They further support the development of full length IGFBP-2 as a cancer therapeutic.

Downloaded from molpharm.aspetjournals.org at ASPET Journals on April 22, 2024

Molecular Pharmacology Fast Forward. Published on November 23, 2005 as DOI: 10.1124/mol.105.016998
This article has not been copyedited and formatted. The final version may differ from this version.

Insulin-like growth factor-1 (IGF-1) is a well-recognized survival factor thought to play a key role in anti-apoptotic and mitogenic signaling in cancer. The IGF-1 receptor (IGF-1R) acting through PI 3-kinase/Akt signaling pathways has been linked to enhanced cell growth and tumorigenesis (Rosenzweig, 2004). In this regard, the IGF-binding proteins (IGFBPs) are a class of six soluble proteins exhibiting high affinity for the IGFs capable of reducing IGF-1R activation via sequestration (Rosenzweig, 2004). Over the last few years, studies have demonstrated that IGFBP-3 (Imai et al., 2000) and IGFBP-2 (Dong et al., 2002) have intrinsic biologic activities independent of their IGF sequestration abilities. This is further complicated with respect to IGFBP-2, which has been reported to have opposite effects on normal versus cancer cells (Moore et al., 2003). In addition, a number of *in vitro* studies using colon, adrenal, and prostate cancer cell lines have revealed a positive association between cell proliferation and IGFBP-2 expression (Hoeflich et al., 2001). Consequently, one must test the actions of the IGFBPs in each system to determine whether they exhibit IGF-1 dependent or independent effects.

The six IGFBPs each contain three distinct domains. The N-and C-termini are highly conserved, and contain 16-18 cysteine residues, forming 8-9 disulfide bonds (Rosenzweig, 2004). Based on their disulfide-bonding pattern, the IGFBPs are thyroglobulin type-1 domain homologues (Guncar et al., 1999). NMR spectroscopy and X-ray crystallography have confirmed these domains in IGFBP-6 (Bach et al., 2005) and IGFBP-1 (Sala et al., 2005), respectively. Notwithstanding their structural homologies, a consensus understanding of the IGF-binding domain on the IGFBPs remains elusive. Previous studies indicated that a key IGF-1 binding site on IGFBP-2 is located within its C-terminus (Carrick et al., 2005; Forbes et al., 1998; Ho and Baxter, 1997; Mark et al., 2005; Shand et al., 2003; Wang et al., 1988) while both the N- (Hong

Downloaded from molpharm.aspetjournals.org at ASPET Journals on April 22, 2024

Molecular Pharmacology Fast Forward. Published on November 23, 2005 as DOI: 10.1124/mol.105.016998
This article has not been copyedited and formatted. The final version may differ from this version.

et al., 2002; Imai et al., 2000; Kalus et al., 1998; Zeslawski et al., 2001) and C-termini (Galanis et al., 2001) of IGFBP-3 have been implicated in IGF binding. Studies have also shown the need for both the N- and C-termini of IGFBP-2 (Carrick et al., 2001), IGFBP-3 (Payet et al., 2003), and IGFBP-6 (Bach et al., 2005) for IGF-1/2 binding.

As an initial step in designing small molecular weight, IGFBP-based agents that antagonize IGF action, we are analyzing the structure of the IGF-binding site on IGFBP-2. Photoaffinity-labeling experiments revealed the photoincorporation of two different Gly^{1}-labeled IGF-1 photoprobes at two C-terminal sites within human IGFBP-2 (212-227 and 266-287), on either side of its CWCV motif (residues 247-250; Fig. 1) (Horney et al., 2001). These findings were consistent with other reports (Carrick et al., 2001; Forbes et al., 1998; Shand et al., 2003), indicating a role for the C-terminal thyroglobulin type-1 domain fold in IGF binding (See legend to Fig. 1 for details). Recent NMR analysis of IGFBP-6 could not resolve the distal C-terminus, suggesting it lacked structure and was likely unimportant in IGF binding (Bach et al., 2005). To resolve whether residues downstream of the CWCV motif of IGFBP-2 contribute to IGF-binding, we utilized the tryptophan-specific cleavage reagent, BNPS-skatole (Fontana, 1972). This reagent is ideally suited for use with IGFBP-2 as it contains a single tryptophan residue, located within its CWCV motif. Furthermore, this cleavage site exists outside the disulfide-bonding pattern, essential to maintaining the tertiary structure of this protein. To determine the affinity of the BNPS-skatole products, we have expressed and purified IGFBP-2_{1-248} and IGFBP-$2_{249-289}$, as well as IGFBP-2_{1-190}, as N-terminal GST-fusion proteins in *Escherichia coli.* In addition, human IGFBP-2 with an N-terminal hexahistidine-tag (6His) was expressed in *E. coli* as a control.

Downloaded from molpharm.aspetjournals.org at ASPET Journals on April 22, 2024

Molecular Pharmacology Fast Forward. Published on November 23, 2005 as DOI: 10.1124/mol.105.016998
This article has not been copyedited and formatted. The final version may differ from this version.

In this study, we generated and purified recombinant IGFBP-2, exhibiting a high affinity for IGF-1 (K_D = 150 pM). Treatment of MCF-7 human breast cancer cells with recombinant IGFBP-2 inhibited both IGF-1 stimulated and basal cell growth. Cleavage of IGFBP-2 with BNPS-skatole resulted in the predicted products. The functionality of these cleavage products was further tested using recombinant IGFBP-2_{1-248} and IGFBP-$2_{249-289}$. Recombinant IGFBP-2_{1-190} had similar IGF binding properties to IGFBP-2_{1-248} with lower efficacy in blocking IGF-1 binding to the receptor. 6His•IGFBP-2 was generated and shown to have equivalent activities compared to human IGFBP-2 expressed in CHO cells. These data indicate that both the proximal and distal regions of the C-terminus of IGFBP-2 contribute to the structural information important for high affinity IGF-1 binding.

Downloaded from molpharm.aspetjournals.org at ASPET Journals on April 22, 2024

Molecular Pharmacology Fast Forward. Published on November 23, 2005 as DOI: 10.1124/mol.105.016998
This article has not been copyedited and formatted. The final version may differ from this version.

Materials & Methods

Materials. Human recombinant IGF-1 was generously provided by Genentech, Inc. (South San Francisco, CA). The cDNA encoding human IGFBP-2 (Binkert et al., 1989) was obtained from Dr. Jörg Landwehr (Roche Biotech, Basel, Switzerland). DHFR$^-$ CHO cells and the pMT2 mDHFR expression vector were provided by Dr. David Kurtz (Medical University of South Carolina, Charleston, SC). Human IGF-2 was obtained from GroPep (Adelaide, Australia). HPLC columns were from Vydac Instruments (Hesperia, CA). Tissue culture medium was obtained from Sigma-Aldrich Corp., (St. Louis, MO). Tris (2-carboxyethyl) phosphine hydrochloride (TCEP-HCl) and HRP-NeutrAvidin^{TM} were obtained from Pierce Chemical Co., Inc. (Rockford, IL). Restriction enzymes (EcoRI, BamHI, HindIII, SalI, SphI and XbaI) and restriction buffer were obtained from New England BioLabs (Beverly, MA). All oligonucleotides were purchased from IDT, Inc. (Coralville, IA). All other materials were of reagent grade.

Transfection of DHFR$^-$ CHO Cells. The cDNA for human IGFBP-2 (Feyen et al., 1991) was excised from pTZ18R by digestion with EcoRI and ligated into the EcoRI site of pCMV. DHFR$^-$ CHO cells (clone DG44) were transfected with 30 µg pCMV-IGFBP-2 and 2 µg pMT2 containing mDHFR (Kaufman and Sharp, 1982) using the calcium phosphate method (Sambrook et al., 1989). After 24 h, plates were split 1:4 into nucleoside-free F12 medium containing 10% calf serum and maintained until colony formation. Individual clones were isolated by discrete trypsinization and were subsequently expanded and amplified by splitting into successively higher concentrations of methotrexate. An appropriate clone (CHO-IGFBP2) was selected based on its high level of IGFBP-2 secretion into serum free medium over a 24 h window as detected

Downloaded from molpharm.aspetjournals.org at ASPET Journals on April 22, 2024

Molecular Pharmacology Fast Forward. Published on November 23, 2005 as DOI: 10.1124/mol.105.016998
This article has not been copyedited and formatted. The final version may differ from this version.

by Coomassie blue staining and confirmed by anti-IGFBP-2 immunoblot. This clone was maintained at 100 mg/L methotrexate to preserve amplification of the expressed genes.

Purification of IGFBP-2. CHO-IGFBP-2 ells were grown to confluence in roller bottles and subjected to a weekly cycle of 3 days growth in serum containing medium followed by 4 days in serum free medium. Batches of conditioned medium (CM; 400 – 600 mL) were acidified to pH 3-4 with glacial acetic acid, dialyzed, followed by dialysis in distilled water using Spectra/Por 4 membranes (Spectrum, Laguna Hills, CA; 12,000 – 14,000 MW cutoff) to remove salt and IGF-1 and lyophilized. IGF-1-Sepharose columns were prepared using CH-Sepharose (Amersham Biosciences, Piscataway, NJ) according to the manufacturer.

Dialyzed, lyophilized CM was dissolved in 40-45 mL of 50 mM HEPES, pH 7.4 containing 150 mM NaCl (Buffer A). Insoluble material was removed by centrifugation at 3,000 x g for 20 min. Two mL of IGF-1–Sepharose in Buffer A were added and the slurry was incubated overnight at 4^{o}C with agitation. The column was subsequently washed with 100 mL Buffer A followed by 50 mL of 10% Buffer A. Proteins bound to the column were eluted with 15 mL of 0.5 M acetic acid, dried *in vacuo* using a Speed Vac concentrator (Savant Instruments, Inc., Farmingdale, NY) and stored at -20°C until further purification by reversed phase HPLC (RP-HPLC) on a C_4 column equilibrated in 0.1% TFA and eluted with a gradient of acetonitrile.

MALDI-TOF Mass Spectrometry. Proteins were reduced and alkylated using the water-soluble tris-alkylphosphine TCEP as the reducing agent and 4-vinylpyridine (4VP; Sigma) as the alkylating agent as previously reported (Horney et al., 2001). Aliquots (1 mL) of each sample to be analyzed were mixed with a 50 mM solution of α-cyano-4-hydroxycinnamic acid dissolved in 70% acetonitrile (1:5 v/v protein: matrix; Sigma-Aldrich) and 1 µL of this mixture was placed on

Downloaded from molpharm.aspetjournals.org at ASPET Journals on April 22, 2024

Molecular Pharmacology Fast Forward. Published on November 23, 2005 as DOI: 10.1124/mol.105.016998
This article has not been copyedited and formatted. The final version may differ from this version.

a gold-coated, stainless steel sample plate and air dried. The samples were analyzed using an Applied Biosystems (Framingham, MA) Voyager-DE matrix-assisted laser desorption/ionization (MALDI) time-of-flight (TOF) mass spectrometer equipped with a 337 nm nitrogen laser. A delayed extraction source was operated in linear mode (1.2 m ion flight path, 20 kV accelerating voltage) to acquire the mass spectra. Between 100 and 120 mass scans were averaged to obtain one mass spectrum. Instrumental resolution in linear mode with delayed extraction was approximately 700 (full width at half maximum) at m/z 1297.5. External mass calibration was performed using angiotensin I (MW 1297.5) and ACTH clip 7-38 (MW 3660.2) as standards. Mass accuracy was +/- 2 Da/1,000 Da.

Immunoblot Analysis. Samples were dissolved in SDS sample buffer with or without DTT and resolved on 12.5% SDS-polyacrylamide gels using a Hoefer apparatus (Hoefer Scientific Instruments, San Francisco, CA). Following electrophoresis, proteins were transferred to nitrocellulose. The membranes were blocked for 20 min with BLOTTO (5% w/v milk protein in Tris-buffered saline with Tween (TBST); 10 mM Tris, pH 8.0 containing 150 mM NaCl and 0.05% Tween-20), incubated with a commercial antiserum against intact bovine IGFBP-2 from Upstate (Charlottesville, VA) or an anti-C-terminal antiserum (Santa Cruz, Santa Cruz, CA). Blots were developed and quantified with goat anti-rabbit HRP-conjugated antibodies from Chemicon (Temecula, CA) and developed with the ECL reagent from Amersham Biosciences.

MCF-7 Cell Proliferation Assay. MCF-7 cells were grown in 24-well plates in phenol red free RPMI 1640 containing 10% fetal bovine serum. Following a 24 h serum starvation, they were washed with PBS and stimulated with a range of IGF-1 doses, as indicated. IGFBP-2 was added at 20 or 100 nM concentrations. The wash and treatments were repeated at 48 h and the cells

Downloaded from molpharm.aspetjournals.org at ASPET Journals on April 22, 2024

Molecular Pharmacology Fast Forward. Published on November 23, 2005 as DOI: 10.1124/mol.105.016998
This article has not been copyedited and formatted. The final version may differ from this version.

were harvested and counted at 96 h. Average cell numbers as a percent of control (unstimulated cells minus IGFBP-2) for triplicate wells was determined.

IGFBP-2 Binding Assay. IGFBP-2 binding assays were carried out using polyethylene glycol (PEG) precipitation and centrifugation (McCusker et al., 1988). IGFBP-2 (1 or 4 ng), 6His•IGFBP-2 (4 ng), IGFBP-2_{1-248} (100 ng), or IGFBP-2_{1-190} (100 ng) was combined with various concentrations of IGF-1 ranging from 30 fM to 100 nM in binding assay buffer (100 mM HEPES pH 7.4, 44 mM $NaHCO_3$, 0.01% BSA, 0.01% Triton X-100, 0.02 % NaN_3) followed by addition of 10 nCi ^{125}I-IGF-1 (Amersham). After a 4 h incubation at 23°C (or overnight incubation at 4°C), 250 µL of 0.5% bovine gamma globulin was added followed by 500 µL 25% PEG (avg. MW 8000; Sigma-Aldrich). The samples were incubated for 10 min at 23°C and centrifuged 3 min at 13,000 rpm. The pellets were washed with 1 mL 6.25% PEG and bound radioactivity was quantified in a Compugamma spectrometer (LKB-Wallac, Turku, FN). Counts bound in the presence of 1 µM IGF-1 (non-specific binding) were subtracted to obtain specific binding.

BNPS-skatole Cleavage of IGFBP-2. Fifty µg of IGFBP-2 were dissolved in 0.1 M acetic acid. BNPS-skatole (2 mg; 2-(2'nitrophenylsulfenyl)-3-methyl-3 bromoindolenine; Pierce) was dissolved in 1.5 mL glacial acetic acid (0.333 mg/mL), and 150 µL were mixed with 50 µL of IGFBP-2. The reaction mixture was incubated in a hybridization oven for 3 h at 47°C in the dark. *Extraction:* 200 µL of water were added to the reaction mixture, which was vortexed and centrifuged at 13,000 rpm for 3 min. The supernatant was saved and the pellet was re-extracted in 500 µL of 0.1 M acetic acid, vortexed and centrifuged as above. The supernatants were combined, vortexed, centrifuged, and dried *in vacuo* in a Speed Vac concentrator. The dried

Downloaded from molpharm.aspetjournals.org at ASPET Journals on April 22, 2024

Molecular Pharmacology Fast Forward. Published on November 23, 2005 as DOI: 10.1124/mol.105.016998
This article has not been copyedited and formatted. The final version may differ from this version.

protein was re-extracted in 200 µL of 0.1 M acetic acid, followed by vortexing and centrifugation. The supernatant was dried *in vacuo* and stored at –20°C until further use.

Analysis of BNPS-skatole Cleavage Reaction Products. The BNPS-skatole reaction products from a 300 µg reaction were reconstituted in 100 µL of 0.1% acetic acid, 220 µL 0.5% trifluoroacetic acid (TFA), and 1 µL of 100% TFA. This was then injected onto a C_4 column equilibrated in 0.1% TFA at a flow rate of 1 mL/min. After 10 min, a linear gradient of 0-60% acetonitrile was developed over 60 min to elute the reaction products. Fractions from each peak were collected and dried *in vacuo*, boiled in SDS sample buffer and resolved on a 12.5% non-reducing polyacrylamide gel. Proteins were transferred to an Immobilon-P^{sq} microporous polyvinylidene fluoride (PVDF) membrane (Millipore; Bedford, MA) as described above. The membrane was briefly rinsed with dH_2O, saturated with 100% methanol, and stained with Coomassie brilliant blue (0.1% Coomassie blue R-250 in 1% acetic acid, 40% methanol and 12.5% trichloroacetic acid) at 23°C for 30 min. The membrane was destained in 50% methanol. Bands were excised and sequenced by Edman degradation, using a gas-phase sequencer (ABI 377), in the Protein Sequencing and Peptide Synthesis Facility-Biotechnology Resource Laboratory (Medical University of South Carolina).

MALDI-TOF-MS of BNPS-skatole Reaction Products. Dried HPLC fractions of the BNPS-skatole reaction products were dissolved in 30 µL of 0.1% TFA containing 60% acetonitrile. 0.5 µL-aliquots of each fraction or of recombinant protein were mixed with 1.5 µL of 50 mM α-cyano-4-hydroxycinnamic acid in 0.1% TFA and 70% acetonitrile. The mixture was spotted onto a gold-coated, stainless steel plate, air-dried and analyzed using a PerSeptive Biosystems Voyager-De MALDI-TOF mass spectrometer as detailed above. External mass calibrations were

Downloaded from molpharm.aspetjournals.org at ASPET Journals on April 22, 2024

Molecular Pharmacology Fast Forward. Published on November 23, 2005 as DOI: 10.1124/mol.105.016998
This article has not been copyedited and formatted. The final version may differ from this version.

performed using angiotensin I (1297.5 Da), bovine insulin (5734.54 Da), horse apomyoglobin (16952.56 Da) and E. coli thioredoxin (11674.48 Da). Mass accuracy was +/- 0.1%.

Ligand Blot Analysis. In preparation for ligand blot analysis, samples were boiled in SDS sample buffer (125 mM Tris (pH 6.95) containing 4% SDS, 10 mM EDTA, 15% sucrose, 0.01% bromophenol blue) and resolved on a 12.5% non-reducing polyacrylamide gel. Proteins were transferred to nitrocellulose (MSI Separations, Minnetonka, MN) with a TE-70 SemiPhor apparatus (Hoefer Scientific Instruments) using a one-buffer system (48 mM Tris, 39 mM glycine, 0.0375% SDS and 20% methanol). Transfers were performed at 23^{o}C for 60 min using a constant current of 1.2 mA/cm^{2}. The nitrocellulose was then washed at 23^{o}C for 10 min in Tris-buffered saline (TBS; 150 mM NaCl, 10 mM Tris-HCL, 0.5 g/L NaN_3, pH 7.4) containing 3% NP-40, 1 h in TBS containing 0.2% gelatin, and 5 min in TBS containing 0.1% Tween-20. The nitrocellulose was incubated in TBS with 0.1% Tween-20, 0.5% BSA containing 0.4 µg tetrabiotinylated-IGF-1, $N^{\varepsilon Lys65/68}$(biotin)-IGF-1, or dibiotinylated IGF-2 (Robinson and Rosenzweig, 2004) at 4^{o}C overnight. The membrane was then washed twice in TBS containing 0.2% gelatin at 23^{o}C for 10 min. The blot was incubated for 1 h at 23^{o}C with 8 µg HRP-NeutrAvidin^{TM} (Pierce) in TBS containing 0.2% gelatin. The blot was then exposed to Kodak BioMax MR-1 x-ray film for 1-30 min. To strip blots, the wet blot was placed in 30 mL of stripping buffer (100 mM Tris, pH 6.7, 10% SDS) containing 210 µL β-mercaptoethanol and incubated in a 60^{o}C hybridization oven for 20 min. The stripped blot was washed for 10 min (twice) in TBS with 0.1% Tween-20, followed by blocking for 1 h with BLOTTO at 23°C and probed with the indicated antibody.

Downloaded from molpharm.aspetjournals.org at ASPET Journals on April 22, 2024

Molecular Pharmacology Fast Forward. Published on November 23, 2005 as DOI: 10.1124/mol.105.016998
This article has not been copyedited and formatted. The final version may differ from this version.

IGFBP-2$_{1-248}$ IGFBP-2$_{1-190}$, and IGFBP-2$_{249-289}$ Expression Constructs. IGFBP-2$_{1-248}$ was generated using oligonucleotides 5'-CGC GGA TCC GAG GTG CTG TTC CGC TGC-3' and 5'-CCG GAA TTC TTA CCA GCA CTC CCC ACG CTG-3'. IGFBP-2$_{1-190}$ was generated using oligonucleotides 5'-CGC GGA TCC GAG GTG CTG TTC CGC TGC-3' and 5'-CCG GAA TTC TTA GGG AGT CCT GGC AGG GGG-3'. Polymerase chain reaction (PCR) was performed using the following PCR conditions: initial duration at 95^{o}C for 2 min followed by 30 cycles of 95^{o}C for 30 min, 60^{o}C for 30 sec, and 72^{o}C for 60 sec. The various IGFBP-2 mutants were cloned without the signal peptide-encoding sequence into the pGEX 6P-1 vector (Amersham) between the BamHI and EcoRI restriction sites in the multiple-cloning site.

IGFBP-2$_{249-289}$ was generated using oligonucleotides 5'-GAT CCT GTG TGA ACC CCA ACA CCG GGA AGC TGA TCC AGG GAG CAC CCA CCA TCC GCG GCG ACC CAG AGT GTC ATC TCT TCT ACA ATG AGC AGC AGG AGG CTT GCG GTG TGC ACA CCC AGC GGA TGC AGT AGG -3' and 5'-GAC ACA CTT GGG GTT GTG GCC CTT CGA CTA GGT CCC TCG TGG GTG GTA GGC GCC GCT GGG TCT CAC AGT AGA GAA GAT GTT ACT CGT CGT CCT CCG AAC GCC ACA CGT GTG GGT CGC CTA CGT CAT CCT TAA -3'. These oligonucleotides were annealed using the following PCR conditions: initial duration at 95^{o}C for 30 sec followed by 29 cycles of 53^{o}C for 45 sec, and 72^{o}C for 90 sec. The annealed DNA was incubated with DNA Polymerase I Large Fragment (Klenow; New England Biolabs) in order to fill in the 3'ends. The PCR products were blunt-ended using Zero Blunt® TOPO® PCR Cloning Kit (Invitrogen, Carlsbad, CA). A stop codon (TGA) that was introduced during this procedure was changed to GGA using QuickChange® Site-Directed Mutagenesis Kit (Stratagene, Cedar Creek, TX). The mutant was cloned without the signal peptide-encoding

Downloaded from molpharm.aspetjournals.org at ASPET Journals on April 22, 2024

Molecular Pharmacology Fast Forward. Published on November 23, 2005 as DOI: 10.1124/mol.105.016998
This article has not been copyedited and formatted. The final version may differ from this version.

sequence into the pGEX 6P-2 vector (Amersham Biosciences) between the BamHI and EcoRI restriction sites in the multiple-cloning site.

Bacterial Expression. Constructs were transformed into the Origami™ B (DE3) LysS strain of *Escherichia coli* (Novagen, Madison, WI), and the cells were incubated at 37°C in 10 mL Luria-Bertoni medium containing 50 µg/mL ampicillin and 1 g/100 mL glucose. After a 100-fold dilution into fresh Luria-Bertoni/ampicillin, the cells were regrown to midlog phase (E_{600nm} = ~0.6), the expression of the proteins, as glutathione-S-transferase fusion proteins, was induced by addition of 1 mM isopropyl β-D-thiogalactoside at 37°C for 2-3 h. Cells were harvested by centrifugation at 4,000 rpm for 20 min. The samples were subjected to a freeze-thaw cycle to lyse the cells followed by suspension in lysis buffer. After 15 min incubation on ice, lysis was completed by three 20-sec cycles of sonication with cooling on ice for 20 min to allow for solubilization. Insoluble material was removed by centrifugation at 4000 rpm for 20 min, twice. The protein was expressed originally in the Origami™ B strain of *Escherichia coli*. However, after subsequent tests, we produced the protein in the BL21 (DE3) strain of *E. coli* as a result of higher yields. The protein behaved the same (data not shown).

Purification of IGFBP-2 Fragments. Supernatants from each lysate were incubated at 23°C for 30 min with a 50% slurry of equilibrated glutathione-Sepharose 4B (Amersham Biosciences; 1mL bed volume per 100 mL sonicate). The fusion protein-bound matrix was collected by centrifugation at 500 x g for 5 min and washed three times with 10 bed volumes of PBS. It was further washed 3 times with 10 bed volumes of high (25 mM HEPES, 0.05% NaN_3, 0.5 M NaCl, 0.1% Triton X-100, pH 7.5) and low (25 mM HEPES, 0.05% NaN_3, 0.1 M NaCl, 0.1% Triton X-100, pH 7.5) salt. The matrix was then equilibrated in PreScission™ Protease cleavage buffer

Downloaded from molpharm.aspetjournals.org at ASPET Journals on April 22, 2024

Molecular Pharmacology Fast Forward. Published on November 23, 2005 as DOI: 10.1124/mol.105.016998
This article has not been copyedited and formatted. The final version may differ from this version.

(50 mM Tris-HCl, pH 7.5, 150 mM NaCl, 1 mM EDTA) at 4°C. The residual buffer was removed, and the IGFBP-2 fragments were eluted by release (cleavage) from GST bound to the glutathione-Sepharose 4B beads. For each mL of washed glutathione-Sepharose bed volume, 40 µL (80 units) of PreScission™ Protease (cleaves at Q-G bonds, and is also a GST fusion protein; Amersham) were mixed with 960 µL of cleavage buffer, added to the fusion protein-bound glutathione-Sepharose and gently suspended. It was incubated while nutating at 4°C for 4 h. The eluate, containing the protein of interest, was collected by centrifugation of bulk glutathione-Sepharose matrix at 500 x g for 5 min. 200 µL of IGF-1-Sepharose were added to the eluate and was nutated at 23°C for 1 h. It was then placed at 4°C, nutating overnight, followed by nutating for 1 h at 23°C. It was washed three times at 23°C with AC buffer (50 mM HEPES, 150 mM NaCl, 0.05% NaN_3, pH 7.4) and 0.1X AC buffer. The protein was eluted using 0.5 M acetic acid (except IGFBP-$2_{249-289}$). The truncation mutants were resolved on 12.5% SDS-polyacrylamide gels. Concentrations of the protein were assessed by densitometry of Coomassie-stained SDS gels using NIH-Image (version 1.61). This method was validated by amino acid analysis (to within 9.25%).

6His•IGFBP-2 Expression Construct. pET15b 6His•IGFBP-2 was cloned via PCR using CMV-IGFBP-2 as a template and the following primers: 5'-CGC CTC GAG GTG CTG TTC CGC TGC-3' and 5'-CCG GGA TCC TTA CTG CAT CCG CTG-3'. The PCR product of ~875bp corresponding to the sequence of the mature protein, minus the signal sequence, was gel purified by agarose electrophoresis and digested with XhoI and BamHI. The oligo was then ligated into the pET15b vector (Novagen), which had previously been digested with XhoI and BamHI. Confirmation of the correct clone was made by DNA sequencing.

Downloaded from molpharm.aspetjournals.org at ASPET Journals on April 22, 2024

Molecular Pharmacology Fast Forward. Published on November 23, 2005 as DOI: 10.1124/mol.105.016998
This article has not been copyedited and formatted. The final version may differ from this version.

Bacterial Expression of 6His•IGFBP-2. The 6His•IGFBP-2 construct was transformed into BL21 (DE3) *Escherichia coli*, and the cells were incubated at 37°C in 10 mL Luria-Bertoni medium containing 200 µg/mL ampicillin. After a 100-fold dilution into fresh Luria-Bertoni/ampicillin, the cells were regrown to midlog phase (E_{600nm} = ~0.6), and the expression of the protein was induced by addition of 1 mM isopropyl β-D-thiogalactoside at 37°C for 3 hours. Cells were harvested by centrifugation at 4000 rpm for 20 min. The samples were subjected to freeze-thaw cycle to lyse the cells as described.

Purification of 6His•IGFBP-2. Supernatants from each lysate were incubated at 4°C for 1 h with 50% slurry of equilibrated His-Select™ Nickel Affinity gel (Sigma-Aldrich). The protein-bound beads were collected by centrifugation at 500 x g for 5 min and washed three times with His-equilibration buffer (50 mM sodium phosphate, 0.3 M sodium chloride, pH 8.0). It was further washed 3 times with 10 bed volumes of high (25 mM HEPES, 0.05% NaN_3, 0.5 M NaCl, 0.1% Triton X-100, pH 7.5) and low (25 mM HEPES, 0.05% NaN_3, 0.1 M NaCl, 0.1% Triton X-100, pH 7.5) salt. The beads were then washed three times with 5 mM imidazole in His-equilibration buffer. The protein was eluted with 200 mM imidazole in His-equilibration buffer. After elution, the imidazole was dialyzed away overnight at 4°C against AC buffer. The sample was then collected and placed over IGF-1-Sepharose as detailed above.

IGFBP-2$_{249-289}$ Binding Assay. The indicated concentrations of competing, unlabeled IGFBP-2$_{249-289}$ (0-887 nM) were added to a constant amount of IGFBP-2 (0.3 pM) and ^{125}I-IGF-1 (20,000 cpm; 15 pM). Following an overnight incubation at 4°C, 200 µL of 0.5% bovine gamma globulin were added, followed by 400 µL of 25% PEG. The samples were incubated for 10 min at 23°C and centrifuged for 15 min at 15,000 x g. The pellets were washed with 1 mL of 6.25%

Downloaded from molpharm.aspetjournals.org at ASPET Journals on April 22, 2024

Molecular Pharmacology Fast Forward. Published on November 23, 2005 as DOI: 10.1124/mol.105.016998
This article has not been copyedited and formatted. The final version may differ from this version.

PEG, and bound radioactivity (^{125}I-IGF-1 bound to IGFBP-2) was quantified in a Compugamma spectrometer (LKB-Wallac).

SCC-9 Cell Culture. SCC-9 cells (human squamous cell carcinoma cell line of the tongue) purchased from ATCC (Manassas, VA) were routinely maintained in a 1:1 mixture of Dulbecco's modified Eagle's medium (DMEM)/Ham's F12 medium supplemented with 10% FBS, penicillin/streptomycin (10 mL/L), HEPES (2.38 g/L), sodium bicarbonate (1.176 g/L for F12; 3.70 g/L for DMEM), and hydrocortisone (400 ng/mL) at 37^{o}C in an atmosphere of 95% air, 5% CO_2 in a humidified incubator.

Cell Binding Assays. SCC-9 were grown to 80% confluence, serum starved for 24 h, and washed with HMS +/– (25mM HEPES, 104 mM NaCl, 5 mM $MgCl_2$, 0.01% soybean trypsin inhibitor, 0.2% BSA, and pH 7.4). Treatments included increasing concentrations of IGFBP-2 or fragment (0.1 nM-500 nM) and ^{125}I-IGF-1 (20,000 cpm). Treatments were preincubated at 37^{o}C for 2 h then placed on the cells for 30 min at 23 ^{o}C. The cells were rinsed with HMS +/–. NaOH was added to dissolve the cells, and the radioactivity was quantified in the gamma counter. Assays were conducted with triplicate concentrations and repeated at least 3 times.

Association Kinetics Experiments. These experiments were carried out using PEG precipitation and centrifugation. 4 ng of rhIGFBP-2 or 100 ng of IGFBP-2-truncation mutant was combined with +/- 500 nM IGF-1 in binding assay buffer (200 mM HEPES (pH 6.0) 44 mM NaHCO3, 0.1% bovine serum albumin, 0.01% Triton-X-100, 0.02% NaN_3), followed by 20,000 cpm of ^{125}I-IGF-1. At times 0, 5, 15, 30, 60, 120, 180, 240 min, bovine gamma globulin and PEG were added and was worked up as described in the competition binding assay method above. Assays were conducted with triplicate concentrations and repeated at least 3 times.

Downloaded from molpharm.aspetjournals.org at ASPET Journals on April 22, 2024

Molecular Pharmacology Fast Forward. Published on November 23, 2005 as DOI: 10.1124/mol.105.016998
This article has not been copyedited and formatted. The final version may differ from this version.

Dissociation Kinetics Experiments. These experiments were carried out using PEG precipitation and centrifugation. 4 ng of rhIGFBP-2 or 100 ng of IGFBP-2-truncation mutant was combined with 20,000 cpm of ^{125}I-IGF-1 in binding assay buffer. After 240 min of association, 500 nM IGF-1 was added to each tube = time 0. At times 5, 15, 30, 60, 120, 180, and 240 min, bovine gamma globulin and PEG were added and the samples were worked up as described above. Assays were conducted with triplicate concentrations and repeated at least 3 times.

Downloaded from molpharm.aspetjournals.org at ASPET Journals on April 22, 2024

Molecular Pharmacology Fast Forward. Published on November 23, 2005 as DOI: 10.1124/mol.105.016998
This article has not been copyedited and formatted. The final version may differ from this version.

Results

Production and Validation of IGFBP-2

A representative chromatogram from the final stage of purification is shown in Fig. 2A, including anti-IGFBP-2 immunoblot analysis of the peaks observed (Fig. 2B). As shown in Fig. 2C, MALDI-TOF MS confirmed the presence of a single protein with molecular ion mass 31,453.7 (MW 31,452.7). In addition to the singly charged molecular ion, the doubly and triply charged ions were observed with m/z of 15,729.6 (calculated MW 31,457.2) and 10,487.3 (calculated MW 31,458.9), respectively. A molecular mass of 31,322.7 Da was expected from the nucleotide sequence of the transfected cDNA. Because the protein contains an uneven number of Cys residues, the mass difference may be due to a Cys residue linked to the additional sulfhydryl group (103 Da) (Feyen et al., 1991). IGFBP-2 was pure based on SDS-PAGE and MALDI-TOF-MS. We used an absorbance value of 0.713 for a 1 mg/mL solution of IGFBP-2 in distilled water to quantify all preparations. In addition to full length IGFBP-2, a second species capable of binding IGF-1 based on its isolation from the IGF-1–Sepharose column was identified (IGFBP-2F). This ~16 kDa peak was heterogeneous in content (Fig. 2D) and variably observed. It reacted with a polyclonal IGFBP-2 antiserum (Fig. 2B), and is likely a proteolytic fragment of IGFBP-2 comprised of either the C-terminus based on its lack of staining with a mid-region directed antibody and peptide mapping profile (Horney and Rosenzweig, unpublished observation). Two heavier components, tentatively identified as an IGFBP-2 homodimer (~66 kDa) and an IGFBP-2/IGFBP-2F heterodimer (~47 kDa) were identified (Fig. 2B). These species were absent from immunoblots run under reducing conditions supporting the notion that they are disulfide-linked dimers.

Downloaded from molpharm.aspetjournals.org at ASPET Journals on April 22, 2024

Molecular Pharmacology Fast Forward. Published on November 23, 2005 as DOI: 10.1124/mol.105.016998
This article has not been copyedited and formatted. The final version may differ from this version.

Binding and Biologic Activities of IGFBP-2

We next tested the IGF-1 binding affinity and biologic activity of recombinant IGFBP-2 in soluble binding and cell growth inhibition assays, respectively. IGF-1 had an EC_{50} of ~170 pM when competing with ^{125}I-IGF-1 for binding to IGFBP-2 (Fig. 3A). This indicated a K_D of 150 pM for IGFBP-2, approximately one order of magnitude higher affinity than the IGF-1R. To assess the biologic activity of recombinant IGFBP-2, we tested its ability to inhibit IGF-1 stimulated and basal growth of human MCF-7 breast cancer cells. As shown in Fig. 3B, IGFBP-2 inhibited IGF-1 stimulated MCF-7 cell proliferation at 20 and 100 nM concentrations. The 20 nM dose reduced the effect of a maximal stimulatory dose of IGF-1 (20 nM) by ~50%. 100 nM IGFBP-2 reduced the effect of 20 nM IGF-1 by greater than 80%, to near unstimulated growth levels. The lack of complete growth inhibition may be explained by the presence of an endogenous growth stimulating IGF-2:IGF-1R autocrine loop (Quinn et al., 1996). The existence of an auto-regulatory loop is clearly evident in the samples where no exogenous IGF-1 was added. In this case, basal growth was significantly inhibited by addition of either 20 or 100 nM IGFBP-2 to levels below that seen in control cultures (Fig. 3B). The lack of complete blockade of IGF-1 action may be due to proteolysis of IGFBP-2 by proteinases expressed by the MCF-7 cells (unpublished observations) (Bunn and Fowlkes, 2003).

BNPS-skatole Cleavage of IGFBP-2

Based on the properties of BNPS-skatole and the C-terminal disulfide-bonding pattern of IGFBP-2 (Forbes et al., 1998), we predicted that the BNPS-skatole reaction products would include IGFBP-$2_{1\text{-}248}$ and IGFBP-$2_{249\text{-}289}$ with molecular masses of 26,755.6 Da and 4,585.1 Da, respectively (Fig. 4A). Cleavage of IGFBP-2 with BNPS-skatole was examined by immunoblot and ligand blot analyses (Fig. 4B). Using a C-terminal-specific IGFBP-2 antibody, both intact

Downloaded from molpharm.aspetjournals.org at ASPET Journals on April 22, 2024

Molecular Pharmacology Fast Forward. Published on November 23, 2005 as DOI: 10.1124/mol.105.016998
This article has not been copyedited and formatted. The final version may differ from this version.

IGFBP-2 and IGFBP-$2_{249-289}$ were detected (Fig. 4B panel b). IGFBP-2_{1-248} was not labeled, consistent with the loss of its epitope-containing C-terminus (249-289). IGFBP-$2_{249-289}$ migrated according to its predicted molecular mass of ~5 kDa and was faintly stained. Probing with a polyclonal anti-IGFBP-2 antibody revealed the presence of intact IGFBP-2 and IGFBP-2_{1-248} in the final reaction mixture (Fig. 4B panel c). IGFBP-2_{1-248} migrated more rapidly than intact IGFBP-2, with an apparent electrophoretic mobility of ~29 kDa, consistent with the loss of its C-terminus. The presence of intact IGFBP-2 suggested that the reaction efficiency was considerably less than 100%. To determine the IGF-1 binding activity of the reaction products, ligand blot analysis was employed (Fig. 4B panel d). Intact IGFBP-2, IGFBP-2_{1-248} and IGFBP-$2_{249-289}$ were all detectable by ligand blot, indicating that they retain IGF-1 binding activity.

Sequence Analysis of IGFBP-2 BNPS-skatole Cleavage Reaction Products

To confirm the BNPS-skatole cleavage specificity the reaction products from an IGFBP-2 BNPS-skatole cleavage reaction were separated by RP-HPLC on a C_4 column. Fractions from each peak were collected, resolved by SDS-PAGE, transferred to a microporous PVDF membrane, and stained with Coomassie brilliant blue (data not shown). While intact IGFBP-2 and IGFBP-2_{1-248} co-eluted from the column, IGFBP-$2_{249-289}$ eluted as a single component. To confirm their identities, Edman degradation was performed on each band by gas-phase sequencing. The sequence data obtained matches the predicted results (Table 1). These findings, taken together with the blots shown in Fig. 4, confirm that BNPS-skatole cleaves IGFBP-2 at the C-terminal end of the tryptophan residue in the CWCV motif.

Downloaded from molpharm.aspetjournals.org at ASPET Journals on April 22, 2024

Molecular Pharmacology Fast Forward. Published on November 23, 2005 as DOI: 10.1124/mol.105.016998
This article has not been copyedited and formatted. The final version may differ from this version.

MALDI-TOF MS Analysis of IGFBP-2 BNPS-skatole Cleavage Reaction Products

To further verify the BNPS-skatole cleavage site on IGFBP-2, the reaction products were resolved by RP-HPLC and analyzed by MALDI-TOF MS (data not shown). The MALDI-TOF MS spectrum of one HPLC fraction exhibited a peak at m/z of 31,509.6 (theoretical 31,322.7 Da) corresponding to intact IGFBP-2. A second peak in this HPLC fraction and MALDI-TOF MS spectrum was observed at m/z of 26,806.7. This corresponds to IGFBP-$2_{1\text{-}248}$ (theoretical 26,755.6 Da). The MALDI-TOF MS spectrum of another HPLC fraction exhibited a peak with the strongest signal at m/z of 4,720.0. This corresponds to IGFBP-$2_{249\text{-}289}$ with a theoretical mass of 4,585.1 Da. The differences between the observed and theoretical masses (IGFBP-2 186.9 Da, IGFBP-$2_{1\text{-}248}$ 51.1 Da, IGFBP-$2_{249\text{-}289}$ 134.9 Da) are likely due to modifications caused by BNPS-skatole side reactions. The well known BNPS-skatole-induced modifications include: conversion of methionine to its sulfoxide (+16 Da); oxidation of C-terminal tryptophan (+14 Da); oxidation of internal tryptophan (+16 Da); and bromination of tyrosine (+79 Da; (Rahali and Gueguen, 1999; Vestling et al., 1995)). Furthermore, other studies using BNPS-skatole have reported the inability to account for an increase of 100 Da of a reaction product (Rahali and Gueguen, 1999). As described above, these results confirm that BNPS-skatole cleaved IGFBP-2 at its tryptophan residue.

Expression and Characterization of 6His•IGFBP-2 and IGFBP-2 Truncation Mutants

Although ligand blot analysis provides qualitative assessments of IGF:IGFBP binding interactions, to obtain a quantitative analysis and define affinities, it is necessary to perform competition binding assays. Given the low yields of product formation using BNPS-skatole and the fact that we obtained a number of potential side reactions leading to chemical modifications of IGFBP-2 and its reaction products, we expressed the predicted products of the BNPS-skatole

Downloaded from molpharm.aspetjournals.org at ASPET Journals on April 22, 2024

Molecular Pharmacology Fast Forward. Published on November 23, 2005 as DOI: 10.1124/mol.105.016998
This article has not been copyedited and formatted. The final version may differ from this version.

reaction, as well as IGFBP-$2_{1\text{-}190,}$ as GST-fusion proteins (Fig. 5A; (Shand et al., 2003)). The truncation mutants were sequentially purified on glutathione-Sepharose, eluted by cleavage with PreScission™ protease and subsequently affinity purified on IGF-1-Sepharose (except IGFBP-$2_{249\text{-}289}$). Because we could not express IGFBP-2 as a GST-fusion protein, it was cloned into the pET15b vector with an N-terminal 6His tag. As part of the cloning strategy, a linker containing the amino acids, GPLGS, was added to all expressed proteins. Furthermore, extra amino acids, PGIRGS and SSGLVPRGSHML, were added at the N-terminus of IGFBP-$2_{249\text{-}289}$ and 6His•IGFBP-2, respectively, during the cloning process. The added peptides were reflected in the masses obtained by MALDI-TOF MS analysis. MALDI-TOF MS analysis (Fig. 5B) of the purified proteins revealed masses (m/z) of 33,337.06 (6His•IGFBP-2; theoretical 33,368.0 Da; a), 27,177.5 (IGFBP-$2_{1\text{-}248}$; theoretical 27,167.0 Da; b) and 20,357.7 (IGFBP-$2_{1\text{-}190}$; theoretical 20,359.2 Da; c), and 5,637.1 (IGFBP-$2_{249\text{-}289}$; theoretical 5,634.3 Da; d), consistent with their purity and expected masses.

Downloaded from molpharm.aspetjournals.org at ASPET Journals on April 22, 2024

Molecular Pharmacology Fast Forward. Published on November 23, 2005 as DOI: 10.1124/mol.105.016998
This article has not been copyedited and formatted. The final version may differ from this version.

Ligand Blot Analysis of IGFBP-2, 6His•IGFBP-2 and IGFBP-2 Truncation Mutants

We initially tested the IGF binding activity of the recombinant proteins using ligand blot analysis with biotinylated IGF-1 or IGF-2 (Fig. 6A). Both IGFBP-2_{1-248} and IGFBP-2_{1-190} bound IGF-2 to a greater extent than IGF-1 as reflected by stronger signals. Furthermore, IGFBP-2_{1-248} exhibited greater IGF binding activity than 1GFBP-2_{1-190}. For example, 0.25 µg of IGFBP-2_{1-248} was readily detected with biotinylated IGF-1, while only a faint band was detected using 2.5 µg of IGFBP-2_{1-190}. The difference in the intensities of the bands in Fig. 4B versus Fig. 6B may be due to BNPS-skatole-induced chemical modifications. Importantly, 6His•IGFBP-2 behaved equivalently to mammalian-cell derived IGFBP-2 (20 and 100 ng).

Competition Binding Studies of IGFBP-2, 6His•IGFBP-2 and IGFBP-2 Truncation Mutants

As illustrated in Fig. 6B, IGFBP-2_{1-248} and IGFBP-2_{1-190} exhibited IGF-1 binding affinities of 7 nM and 9.2 nM, respectively, for IGF-1. This represents an approximate 20- and 26-fold loss of binding activity compared to intact IGFBP-2 (EC_{50} of 0.35 nM). These relatively high affinities contrasted with the comparatively weak signals obtained in ligand blot analysis (Fig. 6 A, B), underscoring the qualitative nature of ligand blotting. This difference could be due to the fact that the competition binding assay is performed in solution while in the ligand blot, proteins are immobilized on nitrocellulose paper. 6His•IGFBP-2 (EC_{50} of 0.76 nM) had an affinity for IGF-1 that was comparable to mammalian-cell derived IGFBP-2, indicating that the protein expressed in bacteria was correctly folded. This validates the data collected using proteins expressed in bacteria, with the differences observed being due to altered specificities. To analyze the binding activity of IGFBP-$2_{249-289}$ we had to modify our assay protocol. The assay used PEG

Downloaded from molpharm.aspetjournals.org at ASPET Journals on April 22, 2024

Molecular Pharmacology Fast Forward. Published on November 23, 2005 as DOI: 10.1124/mol.105.016998
This article has not been copyedited and formatted. The final version may differ from this version.

precipitation of IGFBP-2 (~32 kDa) and the fact that free, unbound IGF-1 (7.6 kDa) is not precipitated. Owing to its small mass, IGFBP-$2_{249-289}$ (5.6 kDa) is not precipitated by PEG. Thus, we carried out our standard assay, holding IGFBP-2 and ^{125}I-IGF-1 constant and added increasing concentrations of fragment as competitor (Fig. 6C). In this assay, IGFBP-$2_{249-289}$ exhibited an EC_{50} of 825 nM. This differed from the strong signal obtained in ligand blot analysis (Fig. 4B). It is possible that the BNPS-skatole-induced side reactions preferentially modified IGFBP-$2_{249-289}$ (observed-theoretical difference = 134.9 Da), enhancing its ability to bind or retain bound IGF-1 in the ligand blot while not affecting or even hindering IGF-1 binding to IGFBP-2_{1-248} (observed-theoretical difference = 51.1 Da). In this regard, IGFBP-$2_{249-289}$ lacked binding activity in an immunoprecipitation-based binding assay and when tested in ligand blot analysis (data not shown).

Cell Binding Studies of IGFBP-2, 6His•IGFBP-2 and IGFBP-2 Truncation Mutants

We tested the ability of IGFBP-2, 6His•IGFBP-2, IGFBP-2_{1-248}, IGFBP-2_{1-190} and IGFBP-$2_{249-289}$ to inhibit ^{125}I-IGF-1 binding to the IGF-1R in SCC-9 cells (Fig. 7). IGFBP-2 and 6His•IGFBP-2 significantly inhibited IGF-1 binding to the IGF-1R, with a 10 nM dose causing ~80% and 90% inhibition, respectively (Fig. 7A). IGFBP-2_{1-248} (500 nM) significantly inhibited ^{125}I-IGF-1 binding to the IGF-1R (~65%; Fig. 7B) while IGFBP-2_{1-190} did not significantly inhibit IGF-1R binding at the doses tested. However, there was a trend; as the concentration of IGFBP-2_{1-190} increased, there was a decrease in the ability of ^{125}I-IGF-1 to bind to the IGF-1R. IGFBP-$2_{249-289}$ did not affect IGF-1 binding (Fig. 7B).

Downloaded from molpharm.aspetjournals.org at ASPET Journals on April 22, 2024

Molecular Pharmacology Fast Forward. Published on November 23, 2005 as DOI: 10.1124/mol.105.016998
This article has not been copyedited and formatted. The final version may differ from this version.

Kinetic Studies of IGFBP-2, 6His•IGFBP-2 and IGFBP-2 Truncation Mutants

The inability of IGFBP-2_{1-248} and IGFBP-2_{1-190} to effectively block IGF-1 binding to the IGF-1R suggested a significant difference between these truncation mutants and the full-length protein. Hence we carried out kinetic analyses, comparing the IGF-1 association and dissociation rates for IGFBP-2, 6His•IGFBP-2, IGFBP-2_{1-248} and IGFBP-2_{1-190} (Fig. 8). ^{125}I-IGF-1 associated faster with both truncation mutants compared to IGFBP-2 and 6His•IGFBP-2 ($t_{1/2}$ = 24.7, 25.7, 3.6, and 4.8 min for IGFBP-2, 6His•IGFBP-2, IGFBP-2_{1-248}, and IGFBP-2_{1-190}, respectively; Fig. 8, *left*). These data indicated that loss of residues 249-289 results in a more rapid association with IGF-1. Deletion of residues 191-248 had little further effect on the association/dissociation rates. IGFBP-2 and 6His•IGFBP-2 had similar association/dissociation kinetics. Importantly, IGFBP-2 had significantly slower dissociation kinetics ($t_{1/2}$ = 16 min) than either truncation mutant, with ~72% of the bound IGF-1 remaining after 4 h (Fig. 8, *right*). In contrast, greater than 85% of bound IGF-1 dissociated from IGFBP-2_{1-248} within a $t_{1/2}$ of 2 min. Removal of the remainder of the C-terminus (191-248) had no further effect. The dissociation rate for 6His•IGFBP-2 was similar to IGFBP-2, with ~84% of bound ligand remaining after 4 h.

Downloaded from molpharm.aspetjournals.org at ASPET Journals on April 22, 2024

Molecular Pharmacology Fast Forward. Published on November 23, 2005 as DOI: 10.1124/mol.105.016998
This article has not been copyedited and formatted. The final version may differ from this version.

Discussion

A renewed interest in the role of the IGF system in cancer has surfaced over the last few years with IGF-1/2 having been identified as risk factors in breast, prostate, colon, cervical (Voskuil et al., 2005) and head and neck cancers (Wu et al., 2004). Accompanied by this is the observation that IGFBP-3 is a negative risk factor for cancer (Rosenzweig, 2004). Based on the premise that the IGFBPs represent natural antagonists of the IGFs, our laboratory is developing IGFBP-mimetics as cancer therapeutics, utilizing IGFBP-2 as a template. The role of the IGFBPs in the onset, development, progression and aggressiveness of cancer has been challenged in recent years. This, in large part, is based on accumulating literature demonstrating that some IGFBPs have direct stimulatory or inhibitory actions on tumor cells independent of their IGF sequestering–IGF-1R inhibiting actions. These intrinsic activities vary according to binding protein and whether normal or cancer cells are under examination (reviewed in (Rosenzweig, 2004)). For example, IGFBP-2 was reported to modestly suppress normal prostate cell growth and potently stimulate prostate cancer cell growth (Moore et al., 2003). Lee *et al.* showed that IGFBP-2 enhances the invasion capacity of ovarian cancer cells (Lee et al., 2005) and other groups have shown IGF-independent effects in cancer cells (Hoeflich et al., 2001), including stimulatory effects of IGFBP-2 on MCF-7 cell growth (Chen et al., 1994). As depicted in Fig. 3, we only observed inhibition of IGF-1/2 effects. IGFBP-2 related changes in cell growth/tumorigenicity may be the result of integrin engagement by the RGD motif (Pereira et al., 2004). Significantly, we have not observed any alterations in cell growth by CHO cells overexpressing IGFBP-2.

Downloaded from molpharm.aspetjournals.org at ASPET Journals on April 22, 2024

Molecular Pharmacology Fast Forward. Published on November 23, 2005 as DOI: 10.1124/mol.105.016998
This article has not been copyedited and formatted. The final version may differ from this version.

We observed the dose-dependent inhibition by IGFBP-2 of MCF-7 cell proliferation in response to exogenously added IGF-1. IGFBP-2 inhibited basal MCF-7 cell growth responses, attributable to blockade of an autocrine IGF-2:IGF-1R growth loop (Quinn et al., 1996). It is likely that autocrine release of IGF-2 is responsible for the lack of a 1:1 molar inhibition of exogenous IGF-1 observed, since IGF-2 has a higher affinity for IGFBP-2 than IGF-1 and a lower efficacy at the IGF-1R than IGF-1 (Jones and Clemmons, 1995). These results point to an IGF-dependent mechanism of action for IGFBP-2.

6His•IGFBP-2 represents the first expression of high affinity, full length human IGFBP-2 in bacteria. Our studies indicate that both the *E. coli*- and mammalian cell-derived IGFBP-2 exhibit the same affinities for IGF-1, kinetics of association/dissociation and efficacies for inhibiting ^{125}I-IGF-1 binding to cells. Accordingly, 6His•IGFBP-2 serves as a key control for the truncation mutants expressed in bacteria and validates our analyses using CHO cell-expressed IGFBP-2.

Using BNPS-skatole, a tryptophan-selective cleavage reagent, we obtained initial evidence that the region downstream of the CWCV motif of IGFBP-2 may contribute to high affinity IGF-1 binding activity. Owing to side reactions and low yields, BNPS-skatole was useful for obtaining structural information, but not for functional analysis of the IGFBPs. To further validate these findings, binding analyses were carried out with IGFBP-2$_{1\text{-}248}$ (EC_{50} = 7 nM) which exhibited a ~20-fold reduction in binding activity compared to intact IGFBP-2 (EC_{50} = 0.35 nM). Reports from other laboratories have also documented a role for the C-terminus of IGFBP-2 in IGF binding. Wang *et al.* (Wang et al., 1988) and Ho and Baxter (Ho and Baxter, 1997) demonstrated that C-terminal IGFBP-2 fragments (residues 148-270, 169-289, and 181-289)

Downloaded from molpharm.aspetjournals.org at ASPET Journals on April 22, 2024

Molecular Pharmacology Fast Forward. Published on November 23, 2005 as DOI: 10.1124/mol.105.016998
This article has not been copyedited and formatted. The final version may differ from this version.

exhibit high affinity IGF binding activity. Furthermore, Mark *et al.* (Mark et al., 2005) identified a naturally occurring fragment of IGFBP-2 (167-279) from human plasma having 10% of the IGF-2 binding activity of intact IGFBP-2.

IGFBP-$2_{1\text{-}190}$ had a binding affinity and kinetic properties that were indistinguishable from that of IGFBP-$2_{1\text{-}248}$. The principal differences between these proteins were that IGFBP-$2_{1\text{-}190}$ had a lower capacity to block ^{125}I-IGF-1 binding to cells (Fig. 7B) and yielded a weaker signal in ligand blot analyses (Fig. 6A). The present findings corroborate the N-terminal domain as the site of high affinity IGF binding activity, given the high affinity for IGF-1 exhibited by IGFBP-$2_{1\text{-}190}$ (Siwanowicz et al., 2005). Residues upstream of the CWCV motif have been implicated in IGF binding activity by our lab (Fig. 1; (Horney et al., 2001)) and others. Carrick *et al.* (Carrick et al., 2001) showed that bovine IGFBP-2 (1-185) had a ~48-fold reduction in IGF binding compared to intact IGFBP-2. They recently reported the NMR structure of bovine IGFBP-2 (Carrick et al., 2005), and demonstrated that the C-terminal domain plays a key role in IGF binding and inhibition of IGF binding to the IGF-1R. These results are in keeping with earlier studies that identified residues 222-236 of bovine IGFBP-2 to be important for IGF binding (Fig. 1; (Forbes et al., 1998)). Similarly, mutation of residues Gly 211 and Glu 217 of rat IGFBP-2 resulted in a 4.5-fold reduction in IGF-1 binding activity (Fig. 1; (Shand et al., 2003)). Finally, using NMR analyses, Bach and coworkers (reviewed in Bach et al., 2005), reported that residues upstream of the CWCV motif comprise the IGF-2 binding site within the C-terminal domain of IGFBP-6.

To date, IGF cell binding studies have not been performed using IGFBP-2 fragments. Therefore, we tested the ability of the truncation mutants to inhibit IGF-1 binding to the IGF-1R (Fig. 7).

Downloaded from molpharm.aspetjournals.org at ASPET Journals on April 22, 2024

Molecular Pharmacology Fast Forward. Published on November 23, 2005 as DOI: 10.1124/mol.105.016998
This article has not been copyedited and formatted. The final version may differ from this version.

Although the IGF-1 binding affinity of IGFBP-2_{1-248} was high (EC_{50} = 7 nM), it exhibited a disproportionate loss in its ability to inhibit IGF-1 binding to the IGF-1R compared to IGFBP-2 (10 nM vs. 500 nM). Similarly, IGFBP-2_{1-190} (EC_{50} = 9.2 nM) had a lower ability than that of IGFBP-2_{1-248} to inhibit IGF-1 binding to cells, requiring higher doses to obtain equivalent inhibition. The finding that IGFBP-2_{1-248} and IGFBP-2_{1-190} had reduced abilities to inhibit IGF-1 binding to the IGF-1R on cells compared to full length IGFBP-2 was a surprise, given their high affinities for IGF-1. To explain this discrepancy, we carried out kinetic analyses.

Kinetic studies indicated that the region downstream of the CWCV motif (249-289) provides stability to the IGFBP-2/IGF-1 complex accounting for the slow dissociation rates observed (Fig. 8). Specifically, when present (IGFBP-2), ~72% of IGF-1 remains bound after 4 h of incubation. When deleted (IGFBP-2_{1-248}), ~85% of the bound ligand dissociates within 5 min of incubation. Our results also suggest that the region upstream of the CWCV motif is important for maintaining IGF-1 binding and contributing to binding efficacy. Our data is consistent with the work of Carrick *et al.* (Carrick et al., 2001) who showed that C-terminal deletion mutants of bovine IGFBP-2 (1-185) had faster association and dissociation rates compared to bovine IGFBP-2His (1-279). The similar association/dissociation rates of IGFBP-2_{1-248} and IGFBP-2_{1-190} combined with the cell binding data suggest that the region upstream of the CWCV motif (residues 191-248) contribute to blocking IGF-1 from binding to the IGF-1R. Deletion of the entire C-terminal domain significantly reduces the ability to block IGF-1 action. The equivalent affinity and binding kinetics observed for IGFBP-2 and 6His•IGFBP-2 indicate that the N-terminal 6His tag and linker peptide do not significantly affect IGF-1 binding association, dissociation or efficaciousness.

Downloaded from molpharm.aspetjournals.org at ASPET Journals on April 22, 2024

Molecular Pharmacology Fast Forward. Published on November 23, 2005 as DOI: 10.1124/mol.105.016998
This article has not been copyedited and formatted. The final version may differ from this version.

These data extend our previous findings (Horney et al., 2001) where we demonstrated that the N-terminal Gly^1 residue on IGF-1 contacts the C-terminal domain of IGFBP-2, supporting the C-terminus of IGFBP-2 as an IGF-1 contact site. Using two photoprobes, differing by 3.8 Å (12.8 Å and 9 Å) in spacer length between the Gly^1 α-amino group of IGF-1 and their reactive nitrenes, two contact sites at 212-227 and 266-287 were labeled (Fig. 8A). Sala *et al.* (Sala et al., 2005) reported that His 213, an iron (II)-binding residue of IGFBP-1, is important for IGF-2 binding (Fig. 9a). The equivalent residue in IGFBP-2, Asn 232, resides within ~10.3 Å and ~9.3 Å from residues within the contact sites, measuring from His 221 and Pro 268, respectively (Fig. 9b). This suggests that these two regions may be in close apposition in three-dimensional space and that the Gly^1 residue – which marks the periphery of the IGFBP-binding domain (residues 1-3 and 49-51) – may localize within a pocket delineated by residues 227-241 (residues equivalent to bovine IGFBP-2 222-236; Fig 8A (Forbes et al., 1998)). Fig. 9 demonstrates that IGF-1 can contact the entire C-terminal domain providing a rationale of how loss of the distal C-terminus leads to the observed activities.

In summary, this study has demonstrated that IGFBP-2 acts on MCF-7 cells in an IGF-1 dependent manner, inhibiting IGF-1R stimulated cell proliferation. We also showed that both the distal and proximal regions of the C-terminal domain of IGFBP-2 provide stability and are necessary for inhibiting IGF-1 binding to the IGF-1R, consistent with other IGFBPs (Siwanowicz et al., 2005). These studies support the development of full length IGFBP-2 as a cancer therapeutic. Future studies will focus on chimeric constructs and IGFBP-2 homologues exhibiting protease resistance and lacking integrin engagement actions.

Downloaded from molpharm.aspetjournals.org at ASPET Journals on April 22, 2024

Molecular Pharmacology Fast Forward. Published on November 23, 2005 as DOI: 10.1124/mol.105.016998
This article has not been copyedited and formatted. The final version may differ from this version.

Acknowledgments

We thank Dr. Kevin Schey and the MUSC Mass Spectrometry Facility for assistance with the analysis of IGFBP-2 and IGFBP-2F and Dr. Benjamin Pettus for help in the cell growth inhibition assays.

Downloaded from molpharm.aspetjournals.org at ASPET Journals on April 22, 2024

Molecular Pharmacology Fast Forward. Published on November 23, 2005 as DOI: 10.1124/mol.105.016998
This article has not been copyedited and formatted. The final version may differ from this version.

References

Bach LA, Headey SJ and Norton RS (2005) IGF-binding proteins - the pieces are falling into place. *Trends in Endocrinol Metab* 16:228-234.

Binkert C, Landwehr J, Mary JL, Schwander J and Heinrich G (1989) Cloning, sequence analysis and expression of a cDNA encoding a novel insulin-like growth factor binding protein (IGFBP-2). *EMBO J* 8:2497-2502.

Bunn RC and Fowlkes JL (2003) Insulin-like growth factor binding protein proteolysis. *Trends Endocrinol Metab* 14:176-181.

Carrick FE, Forbes BE and Wallace JC (2001) BIAcore analysis of bovine insulin-like growth factor (IGF)-binding protein-2 identifies major IGF binding site determinants in both the amino- and carboxyl-terminal domains. *J Biol Chem*276:27120-27128.

Carrick FE, Hinds MG, McNeil KA, Wallace JC, Forbes BE and Norton RS (2005) Interaction of insulin-like growth factor (IGF)-I and -II with IGF binding protein-2: mapping the binding surfaces by nuclear magnetic resonance. *J Mol Endocrinol* 34:685-698.

Chen JC, Shao ZM, Sheikh MS, Hussain A, LeRoith D, Roberts CT, Jr. and Fontana JA (1994) Insulin-like growth factor-binding protein enhancement of insulin-like growth factor-I (IGF-I)-mediated DNA synthesis and IGF-I binding in a human breast carcinoma cell line. *J Cell Physiol* 158:69-78.

Dong F, Wu HB, Hong J and Rechler MM (2002) Insulin-like growth factor binding protein-2 mediates the inhibition of DNA synthesis by transforming growth factor-beta in mink lung epithelial cells. *J Cell Physiol* 190:63-73.

Feyen JH, Evans DB, Binkert C, Heinrich GF, Geisse S and Kocher HP (1991) Recombinant human [Cys281]insulin-like growth factor-binding protein 2 inhibits both basal and

Downloaded from molpharm.aspetjournals.org at ASPET Journals on April 22, 2024

Molecular Pharmacology Fast Forward. Published on November 23, 2005 as DOI: 10.1124/mol.105.016998
This article has not been copyedited and formatted. The final version may differ from this version.

insulin-like growth factor I-stimulated proliferation and collagen synthesis in fetal rat calvariae. *J Biol Chem* 266:19469-19474.

Fontana A (1972) Modification of Tryptophan with BNPS-Skatole (2-(2-Nitrophenylsulfenyl)-3-methyl-3-bromoindolenine. *Methods in Enzymol* 25:419-423.

Forbes BE, Turner D, Hodge SJ, McNeil KA, Forsberg G and Wallace JC (1998) Localization of an insulin-like growth factor (IGF) binding site of bovine IGF binding protein-2 using disulfide mapping and deletion mutation analysis of the C-terminal domain. *J Biol Chem*273:4647-4652.

Galanis M, Firth SM, Bond J, Nathanielsz A, Kortt AA, Hudson PJ and Baxter RC (2001) Ligand-binding characteristics of recombinant amino- and carboxyl-terminal fragments of human insulin-like growth factor-binding protein-3. *J Endocrinol* 169:123-133.

Guncar G, Pungercic G, Klemencic I, Turk V and Turk D (1999) Crystal structure of MHC class II-associated p41 Ii fragment bound to cathepsin L reveals the structural basis for differentiation between cathepsins L and S. *EMBO J* 18:793-803.

Ho PJ and Baxter RC (1997) Characterization of truncated insulin-like growth factor-binding protein-2 in human milk. *Endocrinology* 138:3811-3818.

Hoeflich A, Reisinger R, Lahm H, Kiess W, Blum WF, Kolb HJ, Weber MM and Wolf E (2001) Insulin-like Growth Factor-binding Protein 2 in Tumorigenesis: Protector or Promoter? *Cancer Res* 61:8601-8610.

Hong J, Zhang G, Dong F and Rechler MM (2002) Insulin-like growth factor (IGF)-binding protein-3 mutants that do not bind IGF-I or IGF-II stimulate apoptosis in human prostate cancer cells. *J Biol Chem*277:10489-10497.

Downloaded from molpharm.aspetjournals.org at ASPET Journals on April 22, 2024

Molecular Pharmacology Fast Forward. Published on November 23, 2005 as DOI: 10.1124/mol.105.016998
This article has not been copyedited and formatted. The final version may differ from this version.

Horney MJ, Evangelista CA and Rosenzweig SA (2001) Synthesis and characterization of insulin-like growth factor (IGF)-1 photoprobes selective for the IGF-binding proteins (IGFBPs). photoaffinity labeling of the IGF-binding domain on IGFBP-2. *J Biol Chem* 276:2880-2889.

Imai Y, Moralez A, Andag U, Clarke JB, Busby WH, Jr. and Clemmons DR (2000) Substitutions for hydrophobic amino acids in the N-terminal domains of IGFBP-3 and -5 markedly reduce IGF-I binding and alter their biologic actions. *J Biol Chem*275:18188-18194.

Jones JI and Clemmons DR (1995) Insulin-like growth factors and their binding proteins: biological actions. *Endocrine Rev* 16:3-34.

Kalus W, Zweckstetter M, Renner C, Sanchez Y, Georgescu J, Grol M, Demuth D, Schumacher R, Dony C, Lang K and Holak TA (1998) Structure of the IGF-binding domain of the insulin-like growth factor-binding protein-5 (IGFBP-5): implications for IGF and IGF-I receptor interactions. *EMBO J* 17:6558-6572.

Kaufman RJ and Sharp PA (1982) Amplification and expression of sequences cotransfected with a modular dihydrofolate reductase complementary DNA gene. *J Mol Biol* 159:601-621.

Koradi R, Billeter M and Wuthrich K (1996) MOLMOL: a program for display and analysis of macromolecular structures. *J Mol Graph* 14:51-55, 29-32.

Lee EJ, Mircean C, Shmulevich I, Wang H, Liu J, Niemisto A, Kavanagh JJ, Lee JH and Zhang W (2005) Insulin-like growth factor binding protein 2 promotes ovarian cancer cell invasion. *Mol Cancer* 4:7.

Mark S, Kubler B, Honing S, Oesterreicher S, John H, Braulke T, Forssmann WG and Standker L (2005) Diversity of human insulin-like growth factor (IGF) binding protein-2

Downloaded from molpharm.aspetjournals.org at ASPET Journals on April 22, 2024

Molecular Pharmacology Fast Forward. Published on November 23, 2005 as DOI: 10.1124/mol.105.016998
This article has not been copyedited and formatted. The final version may differ from this version.

fragments in plasma: primary structure, IGF-binding properties, and disulfide bonding pattern. *Biochemistry* 44:3644-3652.

McCusker RH, Campion DR and Clemmons DR (1988) The ontogeny and regulation of a 31,000 molecular weight insulin-like growth factor-binding protein in fetal porcine plasma and sera. *Endocrinol* 122:2071-2079.

Moore MG, Wetterau LA, Francis MJ, Peehl DM and Cohen P (2003) Novel stimulatory role for insulin-like growth factor binding protein-2 in prostate cancer cells. *Int J Cancer* 105:14-19.

Payet LD, Wang XH, Baxter RC and Firth SM (2003) Amino- and carboxyl-terminal fragments of insulin-like growth factor (IGF) binding protein-3 cooperate to bind IGFs with high affinity and inhibit IGF receptor interactions. *Endocrinol* 144:2797-2806.

Pereira JJ, Meyer T, Docherty SE, Reid HH, Marshall J, Thompson EW, Rossjohn J and Price JT (2004) Bimolecular interaction of insulin-like growth factor (IGF) binding protein-2 with alphavbeta3 negatively modulates IGF-I-mediated migration and tumor growth. *Cancer Res* 64:977-984.

Quinn KA, Treston AM, Unsworth EJ, Miller MJ, Vos M, Grimley C, Battey J, Mulshine JL and Cuttitta F (1996) Insulin-like growth factor expression in human cancer cell lines. *J Biol Chem* 271:11477-11483.

Rahali V and Gueguen J (1999) Chemical cleavage of bovine beta-lactoglobulin by BNPS-skatole for preparative purposes: comparative study of hydrolytic procedures and peptide characterization. *Journal of Protein Chemistry* 18:1-12.

Downloaded from molpharm.aspetjournals.org at ASPET Journals on April 22, 2024

Molecular Pharmacology Fast Forward. Published on November 23, 2005 as DOI: 10.1124/mol.105.016998
This article has not been copyedited and formatted. The final version may differ from this version.

Robinson SA and Rosenzweig SA (2004) Synthesis and characterization of biotinylated forms of insulin-like growth factor-1: topographical evaluation of the IGF-1/IGFBP-2 AND IGFBP-3 interface. *Biochemistry* 43:11533-11545.

Rosenzweig SA (2004) What's new in the IGF-binding proteins? *Growth Hormone and IGF Research* 14:329-336.

Sala A, Capaldi S, Campagnoli M, Faggion B, Labo S, Perduca M, Romano A, Carrizo ME, Valli M, Visai L, Minchiotti L, Galliano M and Monaco HL (2005) Structure and properties of the C-terminal domain of insulin-like growth factor-binding protein-1 isolated from human amniotic fluid. *J Biol Chem* 280:29812-29819.

Sambrook J, Fritsch E and Mamiatis T (eds) (1989) *Molecular Cloning: A Laboratory Manual*. Cold Spring Harbor Laboratory Press.

Shand JH, Beattie J, Song H, Phillips K, Kelly SM, Flint DJ and Allan GJ (2003) Specific amino acid substitutions determine the differential contribution of the N- and C-terminal domains of insulin-like growth factor (IGF)-binding protein-5 in binding IGF-I. *J Biol Chem* 278:17859-17866.

Siwanowicz I, Popowicz GM, Wisniewska M, Huber R, Kuenkele KP, Lang K, Engh RA and Holak TA (2005) Structural basis for the regulation of insulin-like growth factors by IGF binding proteins. *Structure (Camb)* 13:155-167.

Vestling MM, Kelly MA and Fenselau C (1995) Optimization by Mass Spectrometry of a Tryptophan-specific Protein Cleavage Reaction. *Rapid Commun in Mass Spec* 9:1051-1055.

Downloaded from molpharm.aspetjournals.org at ASPET Journals on April 22, 2024

Molecular Pharmacology Fast Forward. Published on November 23, 2005 as DOI: 10.1124/mol.105.016998
This article has not been copyedited and formatted. The final version may differ from this version.

Voskuil DW, Vieling A, van 't Veer LJ, Kampman E and Rookus MA (2005) The Insulin-like Growth Factor System in Cancer Prevention: Potential of Dietary Intervention Strategies. *Cancer Epidemiology, Biomarkers and Prevention* 14:195-203.

Wang JF, Hampton B, Mehlman T, Burgess WH and Rechler MM (1988) Isolation of a biologically active fragment from the carboxy terminus of the fetal rat binding protein for insulin-like growth factors. *Biochem & Biophys Res Commun* 157:718-726.

Wu X, Zhao H, Do KA, Johnson MM, Dong Q, Hong WK and Spitz MR (2004) Serum levels of insulin growth factor (IGF-I) and IGF-binding protein predict risk of second primary tumors in patients with head and neck cancer. *Clin Cancer Res* 10:3988-3995.

Zeslawski W, Beisel HG, Kamionka M, Kalus W, Engh RA, Huber R, Lang K and Holak TA (2001) The interaction of insulin-like growth factor-I with the N-terminal domain of IGFBP-5. *EMBO J* 20:3638-3644.

Downloaded from molpharm.aspetjournals.org at ASPET Journals on April 22, 2024

Molecular Pharmacology Fast Forward. Published on November 23, 2005 as DOI: 10.1124/mol.105.016998
This article has not been copyedited and formatted. The final version may differ from this version.

Footnotes

a) This work was supported, in part, by a grant from the National Institutes of Health (CA-78887) and a Department of Defense grant to Hollings Cancer Center, (N6311601MD10004) to SAR. MMK was supported by a National Research Service Award from the NIDCR (5F30DE015249) and by the Dental Medicine Scientist Training Program, Colleges of Dental Medicine and Graduate Studies, Medical University of South Carolina. EME was supported by NIH postdoctoral training grant T32 HL07260.

A portion of this work was presented at the 87th Annual Meeting of the Endocrine Society, June 2004, New Orleans, LA.

b) To whom all correspondence should be sent:

Steven A. Rosenzweig, Ph.D.

Department of Cell and Molecular Pharmacology & Experimental Therapeutics

Medical University of South Carolina

173 Ashley Avenue

Post Office Box 250505

Charleston, SC 29425

V: 803-792-5841

F: 803-792-2475

E: rosenzsa@musc.edu

Downloaded from molpharm.aspetjournals.org at ASPET Journals on April 22, 2024

Molecular Pharmacology Fast Forward. Published on November 23, 2005 as DOI: 10.1124/mol.105.016998
This article has not been copyedited and formatted. The final version may differ from this version.

Figure Legends

Figure 1. Primary Sequences of the C-terminal domains of human, bovine, and rat IGBP-2 and human IGFBP-1. Boxed sequences denote consensus CWCV motifs. Gray box encompasses the thyroglobulin type-1 domain. Underlines in human IGFBP-2 are sites (212-227 and 266-287) photoaffinity labeled with IGF-1 (Horney et al., 2001). Open arrowhead indicates the location of the BNPS-skatole cleavage site. Underline in bovine IGFBP-2 denotes the site defined for IGF binding (residues 222-236) (Forbes et al., 1998). Dark arrowheads designate residues (Gly 211 and Glu 217) mutated in rat IGFBP-2 (Shand et al., 2003) resulting in reduced IGF-1 binding activity. Gray arrowhead in human IGFBP-1 denotes His 213 shown to bind to Fe^{2+} which in turn, antagonized IGF-2 binding (Sala et al., 2005).

Figure 2. Purification and analysis of IGFBP-2. Lyophilized CHO-IGFBP2 CM was purified over IGF-1-Sepharose as described in *Methods*. The eluate was dried *in vacuo*, dissolved in 0.1% TFA and injected onto a C_4 column. **A.** A typical elution profile. The bars indicate the peaks collected for analysis. **B.** Fractions 23–27, collected as two separate peaks from the C_4 elution profile shown, were resolved on a 10% SDS gel under non-reducing conditions, transferred to nitrocellulose, and immunoblotted with a polyclonal anti-IGFBP-2 antibody. Intact IGFBP-2 constituted >98% of the peak with R_T 25-26 min by densitometric analysis. An ~15.8 kDa band was detected by immunoblot (IGFBP-2F). **C.** Purified IGFBP-2 was subjected to MALDI-TOF MS analysis as described in *Methods*. Peaks obtained represent the singly $(M+H)^+$, doubly $(M+2H)^{2+}$ and triply $(M+3H)^{3+}$ charged states of the molecular ion, with observed m/z of 31,453.7, 15,729.6 and 10,487.3, respectively. The predicted mass for IGFBP-2 in the singly charged state is 31,322.7. No other peaks were observed. **D.** MALDI-TOF MS

Downloaded from molpharm.aspetjournals.org at ASPET Journals on April 22, 2024

Molecular Pharmacology Fast Forward. Published on November 23, 2005 as DOI: 10.1124/mol.105.016998
This article has not been copyedited and formatted. The final version may differ from this version.

analysis of IGFBP-2F. The mass peaks obtained represent the singly $(M+H)^+$ and doubly $(M+2H)^{2+}$ charged states of one major species with observed mass 15,819.3 and three minor species with observed masses 13,129.9, 12,528.2, and 10,421.8. No other mass peaks were observed.

Figure 3. Competition binding and biologic activity of IGFBP-2. A. IGFBP-2 binding curve. Competition binding assay using increasing doses of IGF-1 in the presence of a fixed amount of ^{125}I-IGF-1 and IGFBP-2. IGFBP-2 (1 ng) was combined with various concentrations of IGF-1 ranging from 30 fM to 100 nM followed by addition of 10 nCi ^{125}I-IGF-1 (15 pM). After a 4 h incubation at 23°C, 250 µL of 0.5% bovine gamma globulin was added followed by 500 µL of 25% PEG. The samples were incubated for 10 min at 23°C and centrifuged 3 min at 13,000 rpm. The pellets were washed with 1 mL 6.25% PEG and bound radioactivity was quantified. Counts bound in the presence of 1 µM IGF-1 (non-specific binding) were subtracted to obtain specific binding. 100% specific binding is the maximum number of counts bound in the absence of competing ligand (IGF-1) after subtraction of non-specific counts. Non-specific counts are counts bound in the presence of a saturating dose of competing ligand (1 µM IGF-1). **B.** Serum-starved MCF-7 cells in 24-well plates were stimulated for 96 h with the indicated concentrations of IGF-1 and IGFBP-2. Cells were trypsinized and counted with a hemocytometer. Shown are average cell numbers for triplicate wells ± SE. Similar results were obtained in at least three separate experiments.

Figure 4. BNPS-skatole cleavage of IGFBP-2. **A.** BNPS-skatole cleaves at the C-terminal end of tryptophan residues (Fontana, 1972). The arrowhead designates the predicted site of cleavage

Downloaded from molpharm.aspetjournals.org at ASPET Journals on April 22, 2024

Molecular Pharmacology Fast Forward. Published on November 23, 2005 as DOI: 10.1124/mol.105.016998
This article has not been copyedited and formatted. The final version may differ from this version.

within the CWCV motif of IGFBP-2. The theoretical masses are based on the amino acid compositions of the respective proteins and peptides. **B.** 20 ng IGFBP-2 (panel a). 10% and 15% of a 10 μg reaction (panels b, c, d). Samples were boiled in SDS sample buffer, resolved by SDS-PAGE, transferred to nitrocellulose and probed with a polyclonal anti-IGFBP-2 antibody (panel a), a site-specific anti-IGFBP-2 C-terminal antibody (panel b) or tetrabiotinylated IGF-1 (panel d)(Robinson and Rosenzweig, 2004). The ligand blot was stripped and reprobed with a polyclonal anti-IGFBP-2 antibody (panel c). The IGFBP-2 C-terminal-specific antibody labeled intact IGFBP-2 and IGFBP-$2_{249-289}$ (panel b). With the polyclonal anti-IGFBP-2 antibody, IGFBP-2 and IGFBP-2_{1-248} bands were heavily labeled (panel c). In the ligand blot (panel d), IGFBP-2, IGFBP-2_{1-248} and IGFBP-$2_{249-289}$ were detected. The autoradiographs shown are representative of at least 3 independent experiments.

Figure 5. Characterization of 6His•IGFBP-2 and IGFBP-2 truncation mutants. A. Schematic of 6His•IGFBP-2, IGFBP-2_{1-248}, IGFBP-2_{1-190}, and IGFBP-$2_{249-289}$ expressed in *E. coli*. **B.** MALDI-TOF MS analysis of 6His•IGFBP-2 (a), IGFBP-2_{1-248} (b), IGFBP-2_{1-190} (c) and IGFBP-$2_{249-289}$ (d). The y-axis is 0-100% ion intensity and x-axis is m/z range 13,000-40,000 for 6His•IGFBP-2 (a), m/z range 12,000-30,000 for IGFBP-2_{1-248} (b), m/z range 8,500-22,000 for IGFBP-2_{1-190} (c) and m/z range 1,500-20,001 for IGFBP-$2_{249-289}$ (d). The mass peaks obtained represent the singly $(M+H)^+$ and doubly $(M+2H)^{2+}$ charged states of the purified protein. The predicted mass for 6His•IGFBP-2, IGFBP-2_{1-248}, IGFBP-2_{1-190}, and IGFBP-$2_{249-289}$ in the singly charged state are 33,368.0 (a), 27,167.0 (b), 20,359.2 (c), and 5,634.3 (d), respectively.

Downloaded from molpharm.aspetjournals.org at ASPET Journals on April 22, 2024

Molecular Pharmacology Fast Forward. Published on November 23, 2005 as DOI: 10.1124/mol.105.016998
This article has not been copyedited and formatted. The final version may differ from this version.

Figure 6. IGF-1 binding activities of IGFBP-2, 6His•IGFBP-2 and IGFBP-2 truncation mutants. A. Ligand Blot and Immunoblot Analyses. IGFBP-2 20 ng (lane 1), 100 ng (lane 2), 6His•IGFBP-2 20 ng (lane 3), 100 ng (lane 4). For IGFBP-2_{1-248} and IGFBP-2_{1-190} the following amounts were loaded: 5 μg, 2.5 μg, 1 μg, 0.5 μg and 0.25 μg. Samples were boiled in SDS sample buffer, resolved by SDS-PAGE, transferred to nitrocellulose and probed with $N^{\varepsilon Lys65/68}$(biotin)-IGF-1, stripped and reprobed with dibiotinylated IGF-2 followed by a polyclonal anti-IGFBP-2 antibody. Autoradiographs shown are representative of at least two independent experiments. **B.** Competition binding assay using increasing doses of IGF-1 in the presence of a fixed amount of ^{125}I-IGF-1 and IGFBP-2**,** 6His•IGFBP-2, IGFBP-2_{1-248} or IGFBP-2_{1-190}. Binding activities were analyzed using a PEG precipitation-based assay to separate bound from free ^{125}I-IGF-1 as described in Methods. IGFBP-2 (4 ng), 6His•IGFBP-2 (4 ng), IGFBP-2_{1-248} (100 ng), or IGFBP-2_{1-190} (100 ng) were combined with various concentrations of IGF-1 (0 to 100 nM) followed by addition of 10 nCi ^{125}I-IGF-1 (15 pM). Maximal binding for IGFBP-2 was 6,000 cpm, 6His•IGFBP-2 was 5,000 cpm, IGFBP-2_{1-248} was 3,000 cpm, and IGFBP-2_{1-190} was 3,000 cpm. Non-specific binding was typically ~250 cpm or less than 9% of total binding. The EC_{50} of IGFBP-2 was 0.35 nM, 6His•IGFBP-2 was 0.76 nM, IGFBP-2_{1-248} was 7 nM, and IGFBP-2_{1-190} was 9.2 nM. Prism version 4 was used to minimize the sum of the squares of the differences from the mean EC_{50} values for each concentration of IGF-1. Assays were conducted with triplicate concentrations and repeated at least 3 times for each protein. **C.** Unlabeled IGFBP-$2_{249-289}$ (0-887 nM) was added to a constant amount of IGFBP-2 (0.3 nM) and ^{125}I-IGF-1 (15 pM). Following an overnight incubation at 4^{o}C, samples were precipitated with PEG as described in Methods. 100% specific binding is the maximum number of counts bound in the absence of competing ligand (IGFBP-$2_{249-289}$) after subtraction of non-specific counts. Non-

Downloaded from molpharm.aspetjournals.org at ASPET Journals on April 22, 2024

Molecular Pharmacology Fast Forward. Published on November 23, 2005 as DOI: 10.1124/mol.105.016998
This article has not been copyedited and formatted. The final version may differ from this version.

specific counts are the counts bound in the presence of a saturating dose of IGF-1 (500 nM). Maximal binding for IGFBP-2 was 3,800 cpm. Non-specific binding was typically ~120 cpm or less than 3% of total binding. The EC_{50} for IGFBP-$2_{249-289}$ was 825 nM. Prism version 4 was used to minimize the sum of the squares of the differences from the mean EC_{50} values for each concentration of IGFBP-$2_{249-289}$. Assays were conducted with triplicate concentrations and repeated 2 times.

Figure 7. Inhibition of IGF-1 Binding to Cells. SCC-9 cells were grown to 80% confluence, serum starved for 24 h, and washed with HMS +/-. Increasing doses of IGFBP-2 (**A**), 6His•IGFBP-2 (**A**), IGFBP-2_{1-248} (**B**), IGFBP-2_{1-190} (**B**) or IGFBP-$2_{249-289}$ (**B**) plus 20,000 cpm of ^{125}I-IGF-1 were incubated at 37^{o}C for 2 h and then added to the cells for 30 min at 23^{o}C. Cells were rinsed, dissolved in NaOH and the radioactivity was quantified by gamma spectrometry. Assays were conducted with triplicate concentrations and repeated at least 3 times. Compared to control *** $p < 0.001$, ** $p < 0.01$, * $p < 0.05$.

Figure 8. IGFBP Binding Kinetics. IGFBP-2 (4 ng), 6His•IGFBP-2 (4 ng), IGFBP-2_{1-248} (100 ng) or IGFBP-2_{1-190} (100 ng) plus 20,000 cpm of ^{125}I-IGF-1 were combined and allowed to bind at 23°C. (*Left*) Association kinetics: At the times indicated, aliquots were taken and the binding was terminated by PEG precipitation and centrifugation. Non-specific binding (counts bound in the presence of 1 μM IGF-1) was subtracted from all samples. (*Right*) Dissociation kinetics: A binding assay was carried out as described above for 240 min, at which time, 500 nM IGF-1 was added to initiate the dissociation experiment (time = 0 min). At the times indicated, aliquots

Downloaded from molpharm.aspetjournals.org at ASPET Journals on April 22, 2024

Molecular Pharmacology Fast Forward. Published on November 23, 2005 as DOI: 10.1124/mol.105.016998
This article has not been copyedited and formatted. The final version may differ from this version.

were taken and binding was terminated by PEG precipitation and centrifugation. Assays were conducted in triplicate and repeated at least 3 times.

Figure 9. Thyroglobulin type-1 domain of IGFBP-2. **a.** Backbone representation of the crystal structure of the C-terminal domain of IGFBP-1 (residues 172-251; PDB ID: 1ZT3); space-filled residue, His 213 (Sala et al., 2005). **b.** Homology model of the thyroglobulin type-1 domain of IGFBP-2 with the major histocompatibility complex (MHC) class II-associated p41 fragment (PDB ID: 1ICF), using Modeller (http://alto.rockefeller.edu/modbase-cgi/). This domain was first described in MHC class II associated p41 Ii fragment bound to cathepsin L (Guncar et al., 1999). The modeled segment is 82 amino acids in length (IGFBP-2 189-270). Asn 232, (space-filled) is the IGFBP-2 equivalent of His 213 in IGFBP-1 (Sala et al., 2005). Space-filled residues, His 221 and Pro 268, are located within the contact sites (212-227 and 266-287) identified by photoaffinity labeling with IGF-1 (Horney et al., 2001). Their distances from Asn 232 are ~10.4 Å and ~9.3 Å, respectively. This figure was prepared using MOLMOL (Koradi et al., 1996).

Downloaded from molpharm.aspetjournals.org at ASPET Journals on April 22, 2024

Molecular Pharmacology Fast Forward. Published on November 23, 2005 as DOI: 10.1124/mol.105.016998
This article has not been copyedited and formatted. The final version may differ from this version.

TABLE 1

Sequence analysis of BNPS-skatole cleaved IGFBP-2

BNPS-skatole-cleaved IGFBP-2 was separated by RP-HPLC on a C_4 column. Fractions from each peak were collected, resolved by SDS-PAGE, transferred to a microporous PVDF membrane, and stained with Coomassie brilliant blue. Each band was subjected to gas-phase sequencing.

Results	**IGFBP-2**	**IGFBP-2$_{1\text{-}248}$**	**IGFBP-2$_{249\text{-}289}$**
Predicted	EVLFRCPPCT	EVLFRCPPCT	CVNPNTGKLI
Sequencing	EVLFRXPPXT	EVLFRXPPXT	XVNPNTGKLI

Downloaded from molpharm.aspetjournals.org at ASPET Journals on April 22, 2024

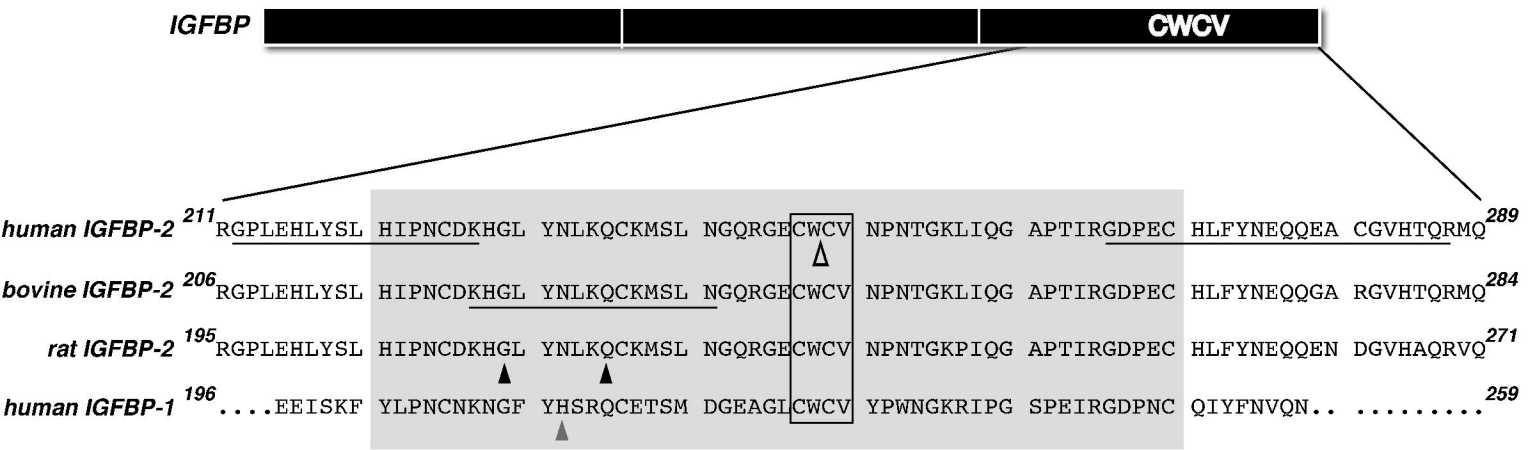
IGFBP
CWCV
human IGFBP-2 211 RGPLEHLYSL HIPNCDKHGL YNLKQCKMSL NGQRGECWCV NPNTGKLIQG APTIRGDPEC HLFYNEQQEA CGVHTQRMQ 289
bovine IGFBP-2 206 RGPLEHLYSL HIPNCDKHGL YNLKQCKMSL NGQRGECWCV NPNTGKLIQG APTIRGDPEC HLFYNEQQGA RGVHTQRMQ 284
rat IGFBP-2 195 RGPLEHLYSL HIPNCDKHGL YNLKQCKMSL NGQRGECWCV NPNTGKPIQG APTIRGDPEC HLFYNEQQEN DGVHAQRVQ 271
human IGFBP-1 196 ....EEISKF YLPNCNKNGF YHSRQCETSM DGEAGLCWCV YPWNGKRIPG SPEIRGDPNC QIYFNVQN.. 259

Figure 1

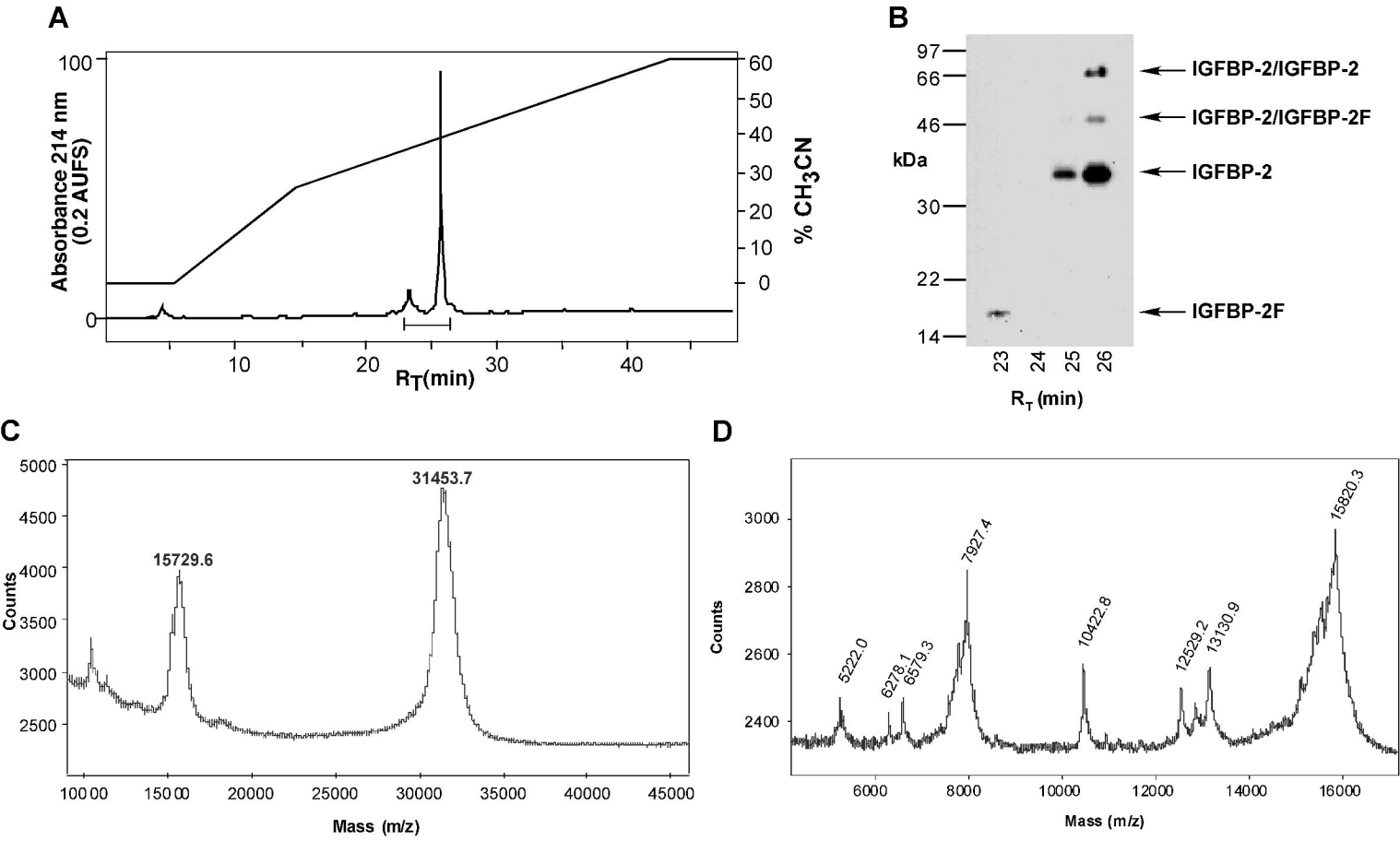
A
Absorbance 214 nm
(0.2 AUFS)
% CH3CN
RT(min)
B
kDa
IGFBP-2/IGFBP-2
IGFBP-2/IGFBP-2F
IGFBP-2
IGFBP-2F
RT (min)
C
15729.6
31453.7
Counts
Mass (m/z)
D
5222.0
6278.1
6579.3
7927.4
10422.8
12529.2
13130.9
15820.3
Counts
Mass (m/z)

Figure 2

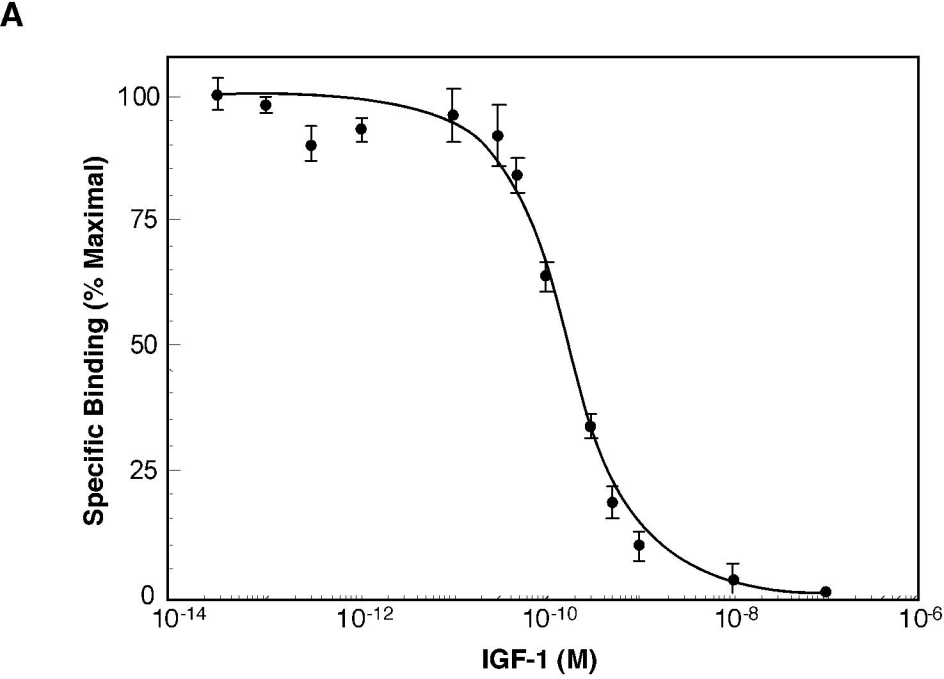
A
Specific Binding (% Maximal)
100
75
50
25
0
10^{-14}
10^{-12}
10^{-10}
10^{-8}
10^{-6}
IGF-1 (M)

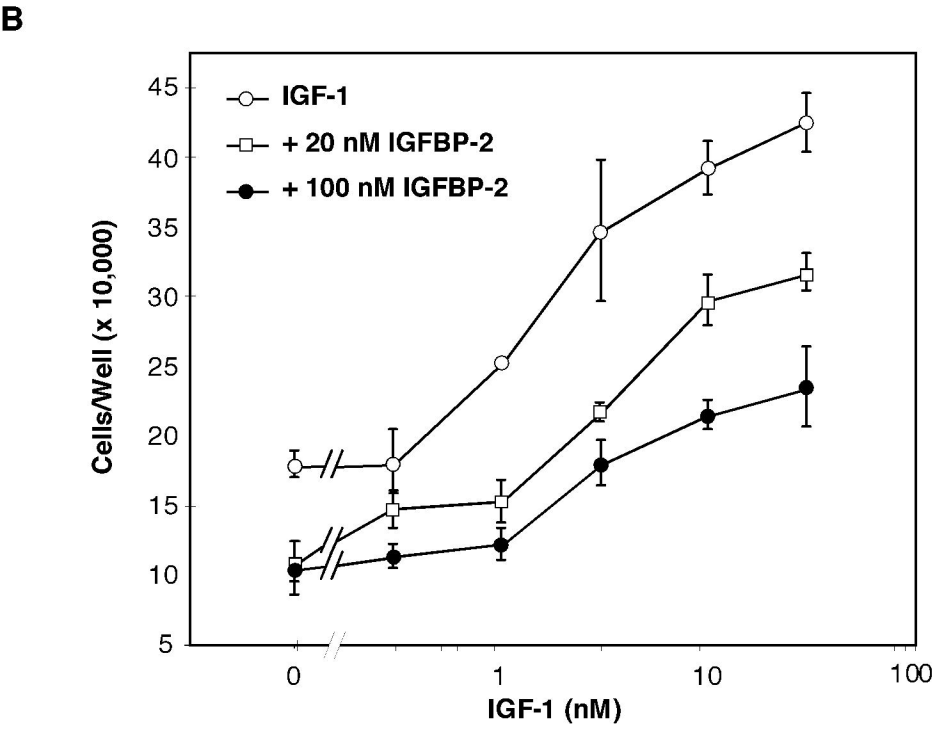
B
IGF-1
+ 20 nM IGFBP-2
+ 100 nM IGFBP-2
Cells/Well (x 10,000)
45
40
35
30
25
20
15
10
5
0
1
10
100
IGF-1 (nM)

Figure 3

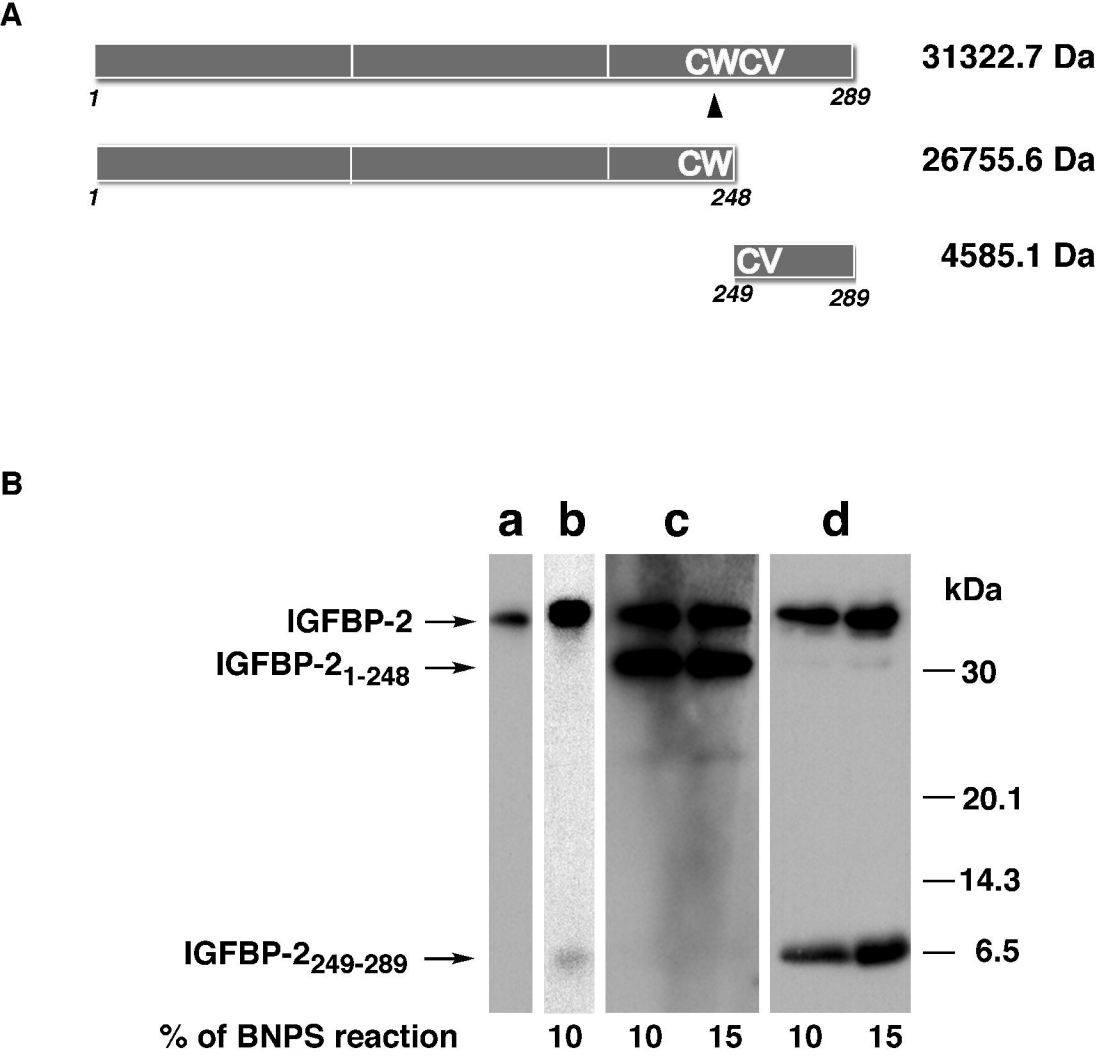

Figure 4

molpharm.aspetjournals.org at ASPET Journals on April 22, 2024

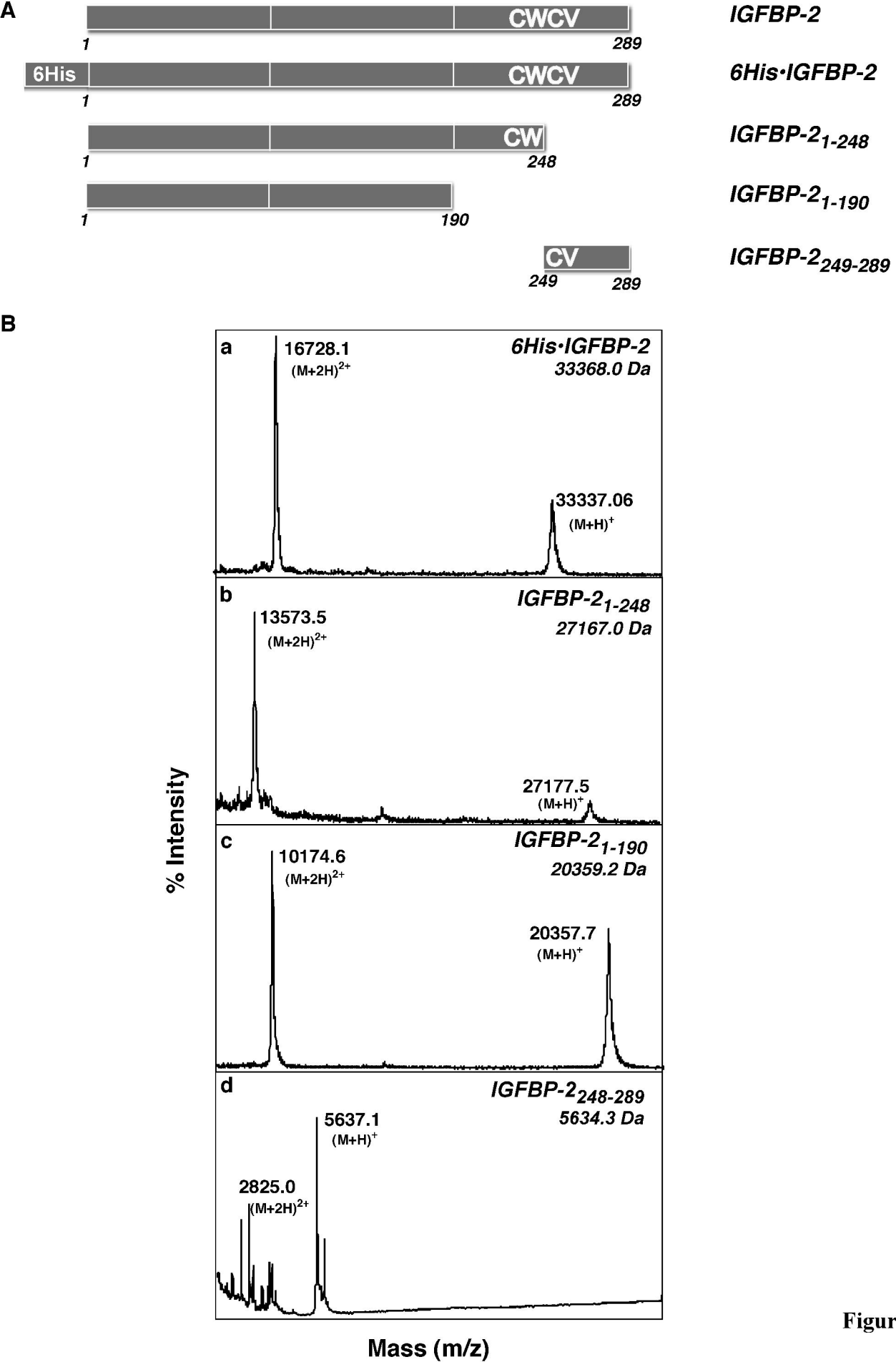
A
CWCV
IGFBP-2
1
289
6His
CWCV
6His·IGFBP-2
1
289
CW
IGFBP-2$_{1-248}$
1
248
IGFBP-2$_{1-190}$
1
190
CV
IGFBP-2$_{249-289}$
249
289
B
a
16728.1
(M+2H)$^{2+}$
6His·IGFBP-2
33368.0 Da
33337.06
(M+H)$^{+}$
b
IGFBP-2$_{1-248}$
13573.5
(M+2H)$^{2+}$
27167.0 Da
27177.5
(M+H)$^{+}$
c
IGFBP-2$_{1-190}$
10174.6
(M+2H)$^{2+}$
20359.2 Da
20357.7
(M+H)$^{+}$
d
IGFBP-2$_{248-289}$
5637.1
(M+H)$^{+}$
5634.3 Da
2825.0
(M+2H)$^{2+}$
% Intensity
Mass (m/z)

Figure 5

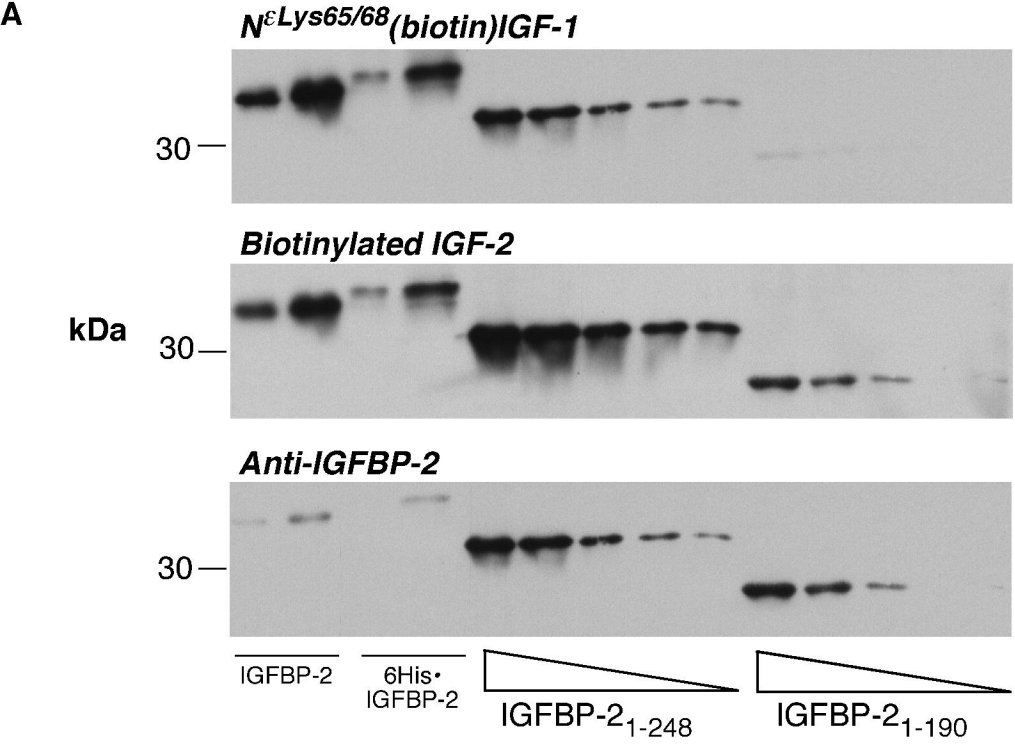
A
Nε Lys65/68 (biotin) IGF-1
30
Biotinylated IGF-2
kDa
30
Anti-IGFBP-2
30
IGFBP-2
6His• IGFBP-2
IGFBP-2 1-248
IGFBP-2 1-190

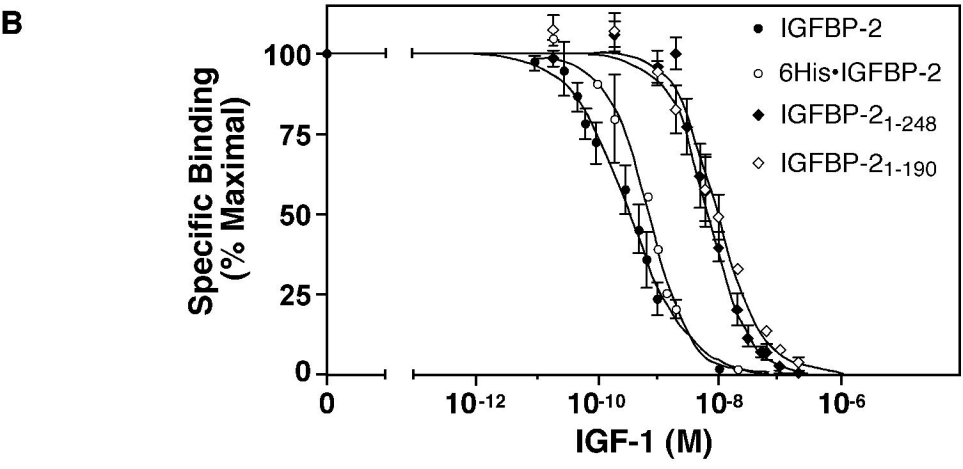
B
Specific Binding (% Maximal)
100
75
50
25
0
0
10-12
10-10
10-8
10-6
IGF-1 (M)
IGFBP-2
6His•IGFBP-2
IGFBP-2 1-248
IGFBP-2 1-190

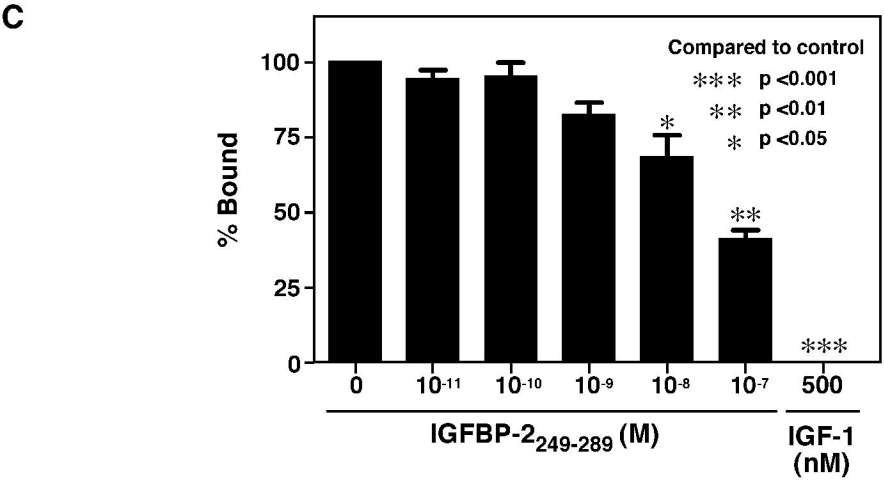
C
% Bound
100
75
50
25
0
Compared to control
*** p <0.001
** p <0.01
* p <0.05
*
**
***
0
10-11
10-10
10-9
10-8
10-7
500
IGFBP-2 249-289 (M)
IGF-1 (nM)

Figure 6

This article has not been copyedited and formatted. The final version may differ from this version.

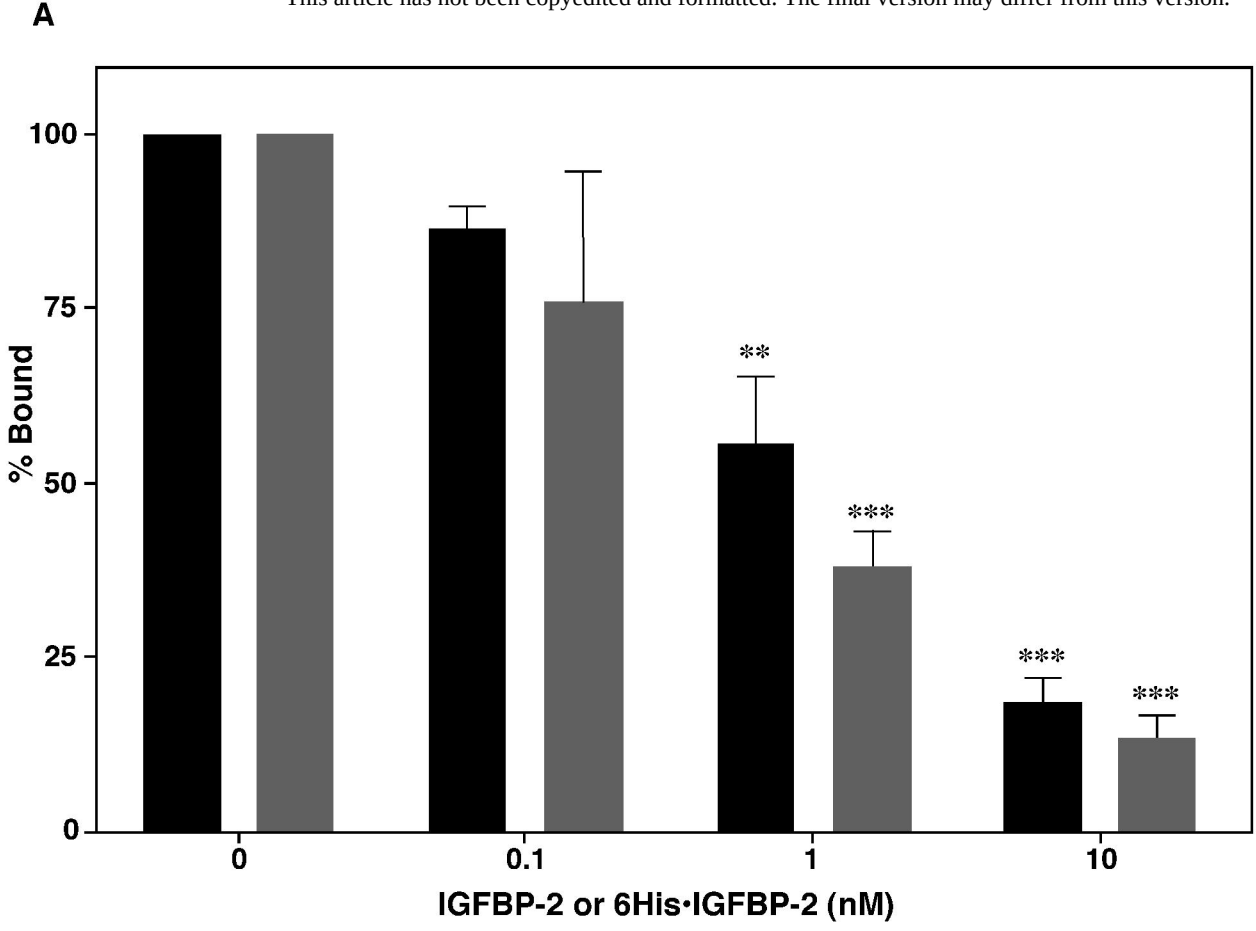

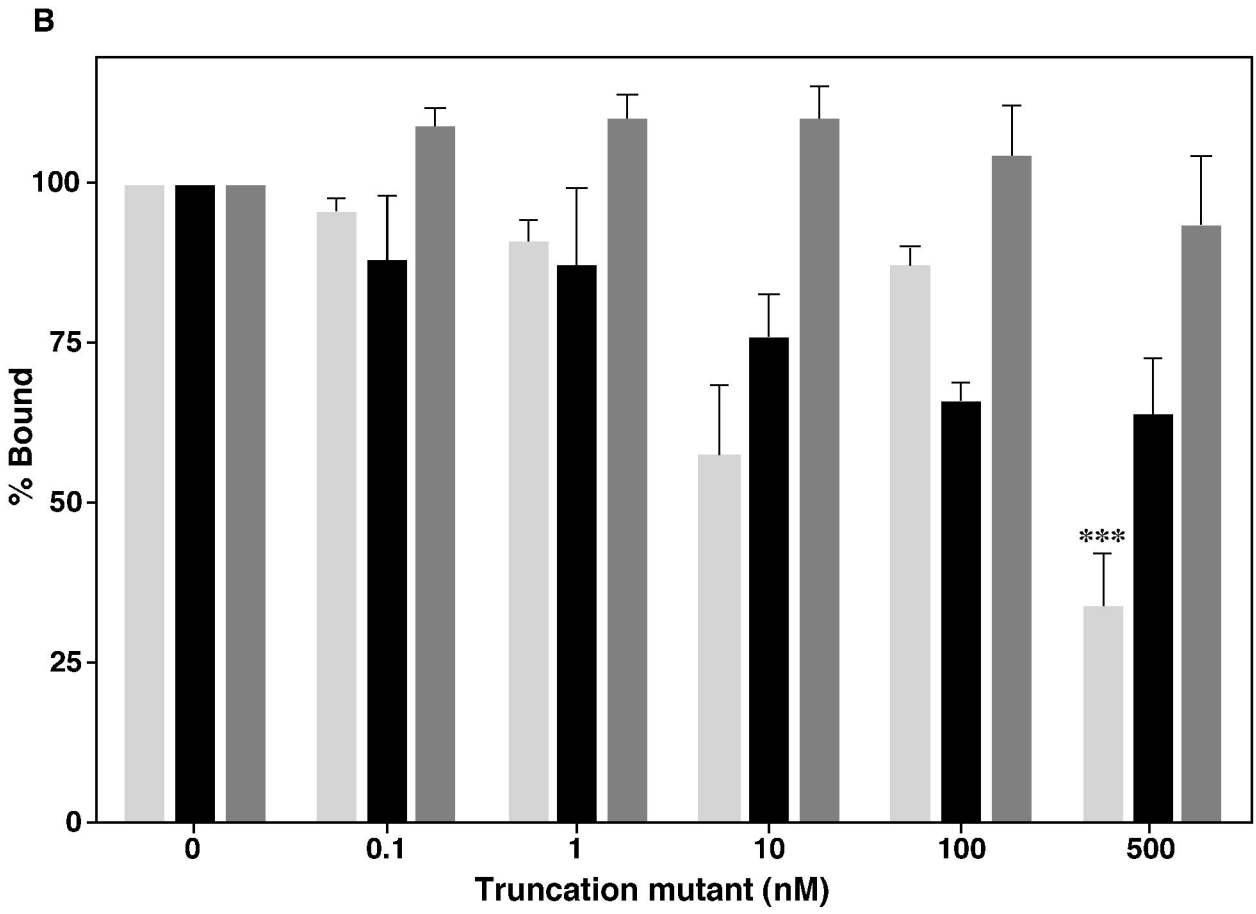

Figure 7

Downloaded from molpharm.aspetjournals.org at ASPET Journals on April 22, 2024

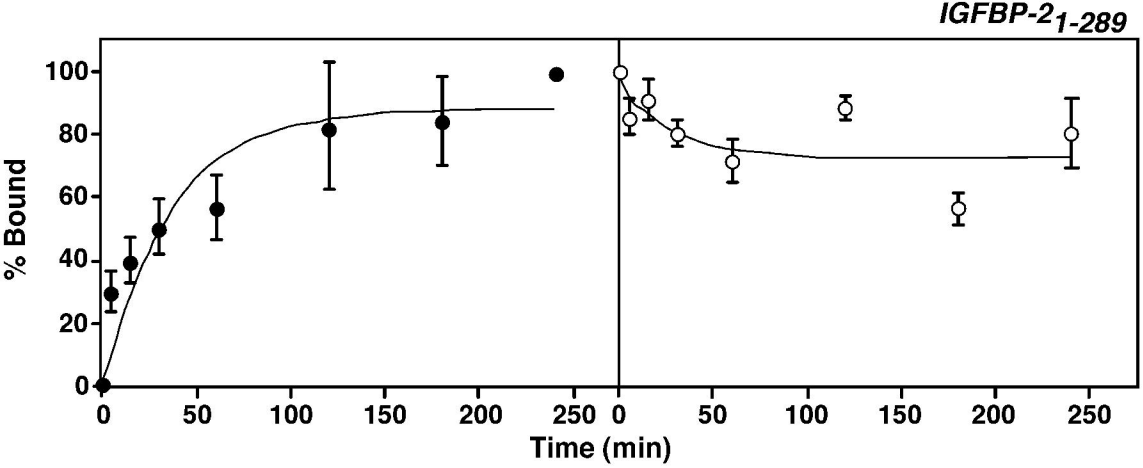
IGFBP-2 1-289
% Bound
Time (min)

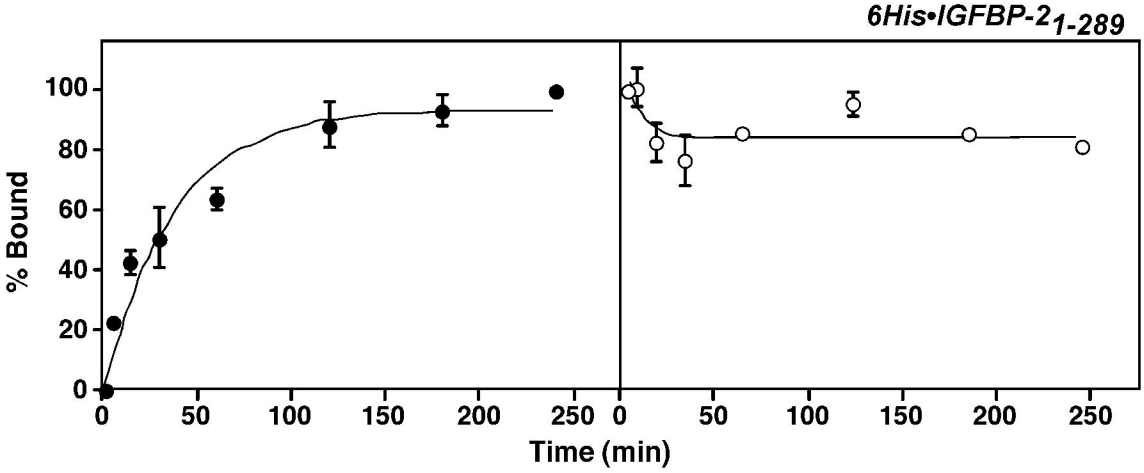
6His•IGFBP-2 1-289
% Bound
Time (min)

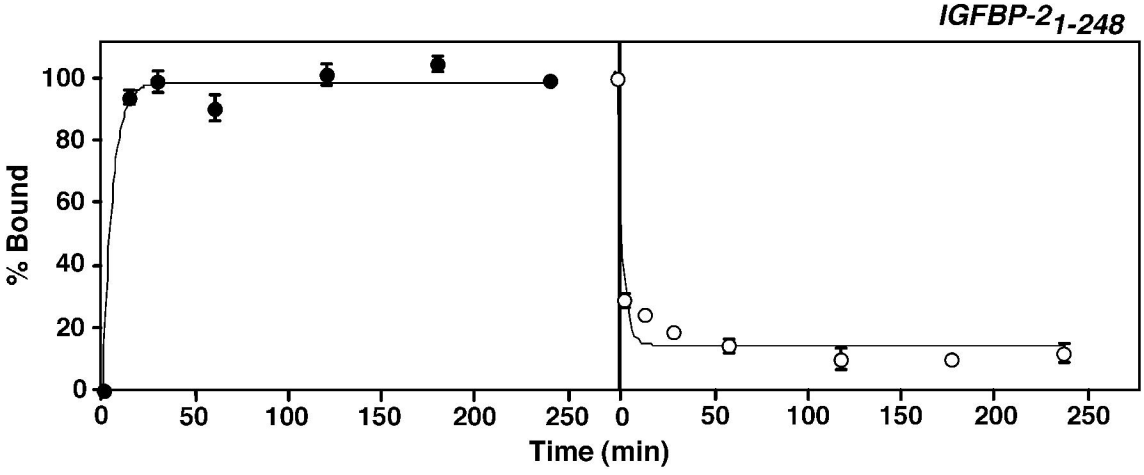
IGFBP-2 1-248
% Bound
Time (min)

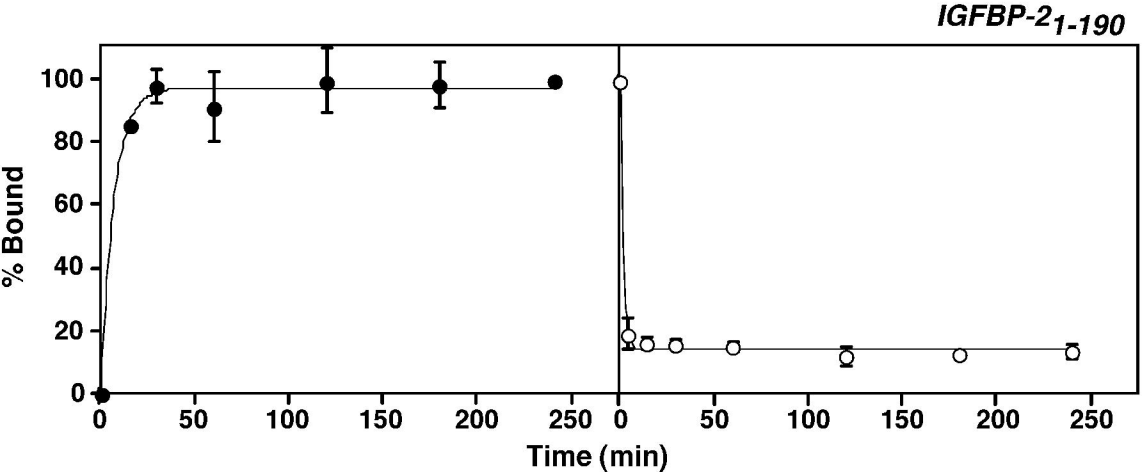
IGFBP-2 1-190
% Bound
Time (min)

Figure 8

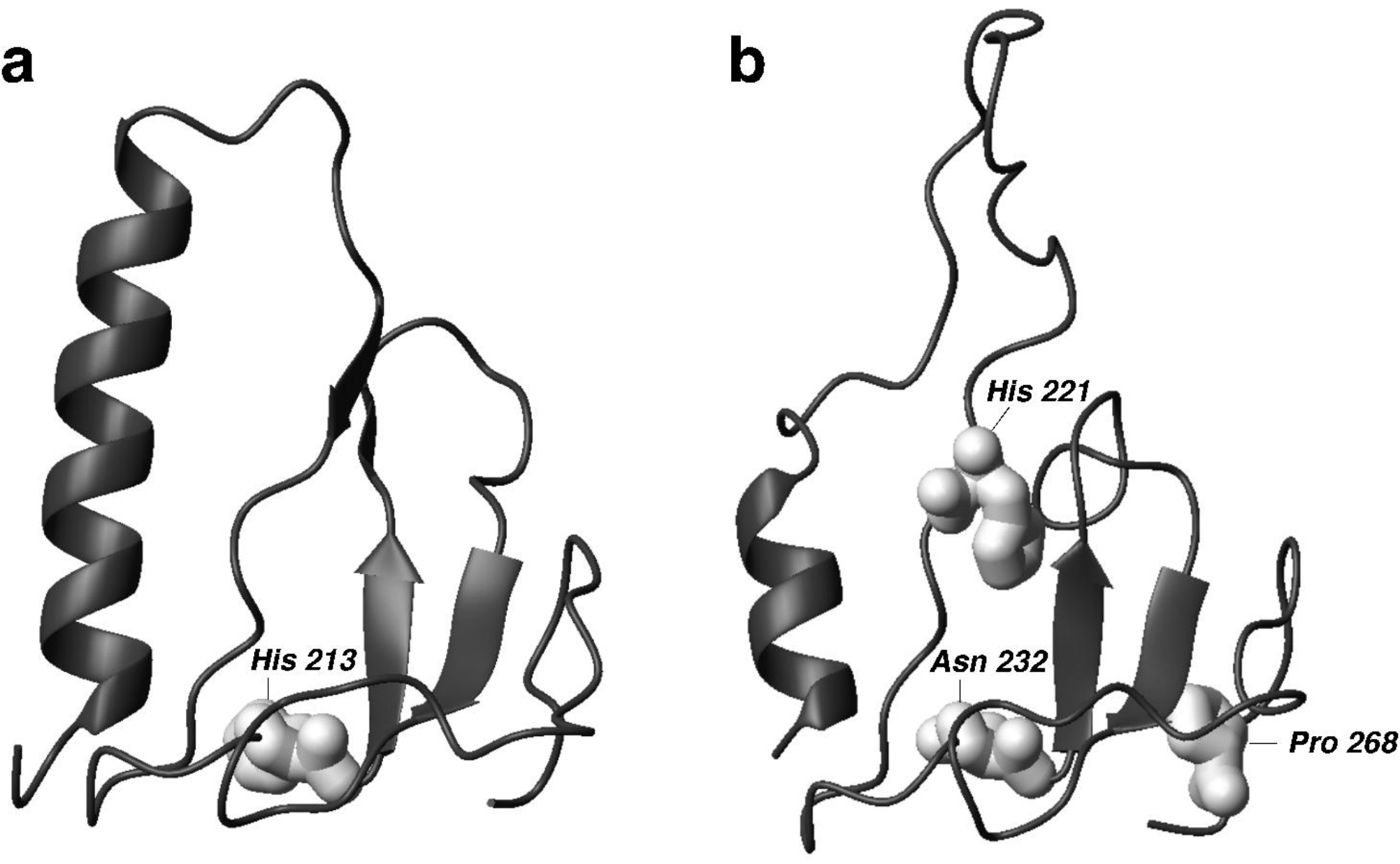

Figure 9